

On a polynomial Alexander invariant for tangles and its categorification

Claudius Zibrowius

Abstract

We generalise the Kauffman state formula for the classical multivariate Alexander polynomial of knots and links to tangles and thereby obtain a finite set of polynomial tangle invariants. In the first part of this paper, we investigate some of their properties; in particular, we show invariance under Conway mutation. Furthermore, we interpret our invariants geometrically in terms of the first homology of the maximal Abelian cover of the tangle complement. As an essential ingredient for this and a useful by-product in general, we prove a generalised version of Kauffman's clock theorem. Finally, we explore two ideas towards a categorification of the polynomial tangle invariants.

Contents

0	Introduction	1
1	The tangle invariant ∇_T^s	5
2	Some basic properties of ∇_T^s	11
3	4-ended tangles and mutation invariance	17
4	Geometric interpretation of ∇_T^s	22
5	Comparison of ∇_T^s to other definitions	26
6	Towards a categorification of ∇_T^s	28
6.1	A naive approach	28
6.2	A categorification via sutured Heegaard Floer theory	36
	Appendix: The proof of the generalised clock theorem	39
	References	45

0 Introduction

The Alexander polynomial of a knot or a link can be defined and interpreted in many different ways, depending on the preferred point of view. For example, this might be geometry/algebra (via Fox calculus, elementary ideals or Reidemeister torsion), combinatorics (via Kauffman states and Alexander codes) or skein theory. However, all of these definitions give essentially the same invariant. It takes the form of a Laurent polynomial in a single variable with integer coefficients. For links, this invariant can be refined to a Laurent polynomial in *several* variables, such that each link component corresponds to a variable. Depending on the context, one sometimes expresses the Alexander polynomial

in different ways by making some cosmetic substitutions. For example, the Conway potential function, which we use for most of this paper, is essentially obtained from the Alexander polynomial by taking the squares of all variables (see remark 1.9).

Recent years have seen an increased interest in generalising the Alexander polynomial to tangles, which can be regarded as “local” knots and links. Again, one can approach this problem from different points of view. In 2010, Archibald used a generalisation of the Alexander matrix to extend the invariant to tangles [Arc10]. In the same year, Polyak gave a skein theoretic description, which also generalises to virtual tangles [Pol10]. Sartori gave a definition of Alexander tangle invariants via representations of $U_q(\mathfrak{gl}(1|1))$ [Srt06]. In 2012, Bigelow found a diagrammatic definition of the one-variable Alexander polynomial that generalises to tangles [Big12]. He used resolutions similar to those in the Kauffman bracket definition of the Jones polynomial, another polynomial knot, link and tangle invariant. Kennedy generalised his formulae to the multivariable case [Ken12].

In this paper, we start from Kauffman’s combinatorial definition of the Conway potential function for knots and links. In section 1, we adapt this definition to tangles. In general, this gives us a finite set of Laurent polynomials, which we call ∇_T^s , associated to an oriented tangle diagram T and some additional input data s that only depends on the tangle itself and not the diagram (see definition 1.5). In theorems 1.7 and 1.8, we show the following result.

Theorem. ∇_T^s is an invariant of the oriented tangle represented by T . Furthermore, if T represents a link or a knot L , there is only one choice for s , namely $s = \emptyset$, and ∇_T^0 is equal to the Conway potential function ∇_L up to a certain factor.

The definition of ∇_T^s is a very straightforward generalisation of Kauffman’s construction, and it is therefore surprising that none of the papers cited above mentions this approach at all. In fact, apart from a short discussion in [GL86], the author is unaware of any reference in the literature.

The invariants satisfy a glueing formula (1.11) which generalises the connected sum formula for the knot and link case. In section 2, we derive some further properties of our tangle invariants. As we will see, many properties of the Conway potential function for knots and links generalise. We show in particular:

Theorem (Propositions 2.1, 2.4, 2.10, 2.11 and corollary 2.5). *Let T be an oriented r -component tangle. Then:*

- If $m(T)$ denotes the mirror image of T , then

$$\nabla_{m(T)}^s(t_1, \dots, t_r) = (\nabla_T^s)(t_1^{-1}, \dots, t_r^{-1}).$$

- If $r(T, t_1)$ denotes the same tangle T with the orientation of the t_1 -strand reversed, then

$$\nabla_{r(T, t_1)}^s(t_1, \dots, t_r) = (-1)^{\text{lk}_T(t_1)} \nabla_T^s(-t_1^{-1}, t_2, \dots, t_r),$$

where $\text{lk}_T(t_1)$ is the sum of all linking numbers of the t_1 -strand with the other components of T (see definition 2.2). Similarly, if $r(T)$ denotes the tangle T with the orientation of all strands reversed, then

$$\nabla_{r(T)}^s(t_1, \dots, t_r) = \nabla_T^s(-t_1^{-1}, \dots, -t_r^{-1}).$$

- If T has a closed component K_1 , then $\nabla_T^s(\pm 1, t_2, \dots, t_r)$ equals $\nabla_{T \setminus K_1}^s(t_2, \dots, t_r)$ up to a certain factor.
- The exponents of a variable t_1 of a closed component K_1 in T is equal to $\text{lk}(t_1) + 1$ modulo 2. There is a more complicated formula for open components.

In section 3, we study ∇_T^s for 4-ended tangles. We show in theorem 3.3:

Theorem. ∇_T^s is a mutation invariant, provided that the open strands of the mutating tangle have the same colour and that if the mutation changes the orientation of those open strands, we also change the orientation of all closed strands in the mutating tangle.

This implies in particular that the *multivariable* Alexander polynomial is a mutation invariant (in the sense of the theorem above), a result for which the author was also unable to find a reference in the literature.

In section 4, we interpret the invariants geometrically in terms of the first homology of the maximal Abelian cover of the tangle complement relative to certain subspaces of its boundary. Because this geometric generalisation of the Alexander polynomial looks even more natural than the one using Kauffman states (but with the slight drawback of being unnormalised), this seems to be a good starting point of any comparisons with aforementioned constructions. In fact, we show in section 5 that in principle, our invariants can be calculated from those defined in [Arc10], and vice versa. However, finding a general closed-form expression for this relationship would require a better understanding of the action of the mapping class group of punctured spheres on our invariants. This would also be helpful for understanding the relation between the Bureau representation for braids and our invariants.

One can place our tangle invariants in a much broader context. In fact, our original motivation comes from Bar-Natan's generalisation of Khovanov homology to tangles [Bar04]. To a tangle diagram, he associates a certain chain complex whose chain homotopy type is a tangle invariant. For knots and links, this invariant can be specialised to Khovanov homology, a graded homology theory which categorifies the Jones polynomial (see for example [Bar02]). The interesting feature of these chain complexes is that they live in a certain category which essentially (that is up to grading) consists of only finitely many objects and morphisms. For example, for 4-ended tangles, there are just two objects and at most four morphisms in each Hom-set.

Knot and Link Floer homology is a homological theory which categorifies the Alexander polynomial [Ras03, OS03, OS07]. Since its discovery, people have found similarities between Khovanov homology and knot Floer homology (see for example [Ras05]). So it is quite natural to look for an analogue to Bar-Natan's construction in knot Floer homology: *What is the local description of knot Floer homology?* Along with a gluing recipe, an answer to this question should be helpful for solving some open problems about knot Floer homology. For example, it is known that Khovanov homology with $\mathbb{Z}/2$ -coefficients is a mutation invariant [Weh09]. The same problem for δ -graded knot Floer homology appears to be still open [BL11, conjecture 1.5].

Thus, the predominant part of this paper can be regarded as an attempt to answer our question on the decategorified level: *What is the ("correct") polynomial local Alexander invariant?* Kauffman's combinatorial definition of the Alexander polynomial (as

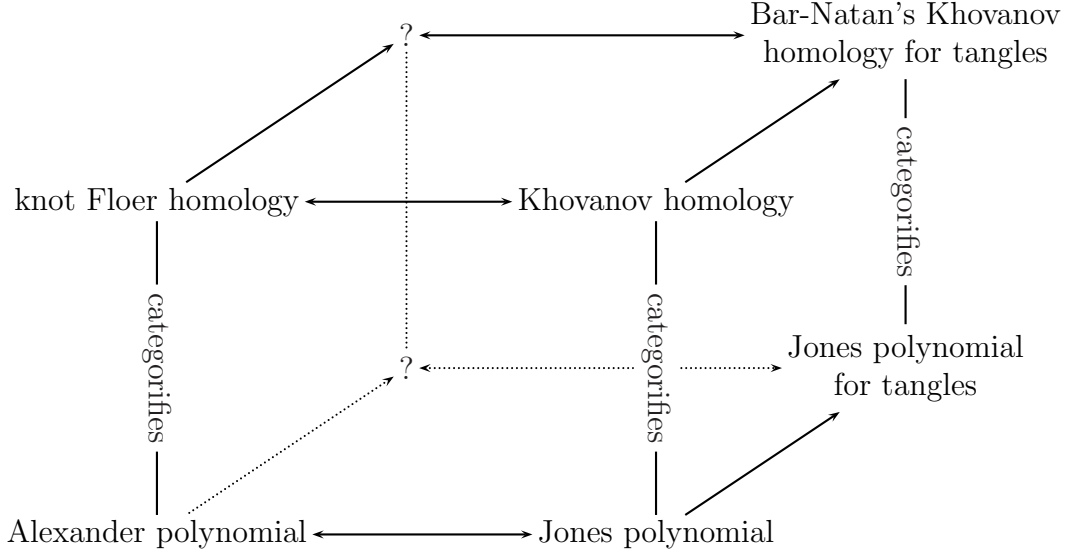


Figure 1: Why is this interesting?

opposed to, say, the one via Alexander matrices) looks very natural for this purpose: It can be used to show that knot and link Floer homology categorifies the Alexander polynomial. (One can also use the skein exact triangle for this.) Of course, a skein theoretic description of the Alexander polynomial for tangles like the one in [Pol10] and [Ken12] seems apter for comparisons with Khovanov homology; however, it is apparently quite hard to guess combinatorial formulae for the differentials.

In the final section 6, we give two different constructions of a homology theory whose Euler characteristic is equal to the polynomial tangle invariant ∇_T^s . The first construction (subsection 6.1) uses a naive notion of Heegaard diagrams for tangles that are basically obtained by intersecting standard Heegaard diagrams for knots and links with 3-balls. Amazingly, this approach works very well for tangles without closed components:

Theorem. *Let T be a tangle without a closed component. To a Heegaard diagram representing T and a site s of T , we can associate a doubly graded chain complex $\widehat{CFT}(T, s)$ whose graded chain homotopy type is independent of the Heegaard diagram and whose graded Euler characteristic is equal to ∇_T^s up to an overall normalisation. If T represents a knot or link L , $\widehat{CFT}(T, \emptyset)$ coincides with ordinary knot or link Floer homology $\widehat{CFL}(L)$.*

In subsection 6.2, we give a shortcut to the previous construction via Juhasz' sutured Floer homology, which also illustrates how to modify the first construction so that it also works for tangles *with* closed components. We prove the following

Theorem. *To a tangle T and a site s , we can associate a sutured 3-manifold X_T^s in a natural way. Then the sutured Floer homology $SFH(X_T^s)$ is an invariant of the tangle T . Furthermore, the Euler characteristic of $SFH(X_T^s)$ is equal to ∇_T^s up to normalisation and an additional factor $(c - c^{-1})$ for each closed component c of T . For tangles without closed components, $SFH(X_T^s)$ coincides with $\widehat{CFT}(T, s)$.*

Recently, Petkova and Vértesi succeeded in constructing a glueable combinatorial tangle Floer homology using grid diagrams and ideas from bordered Floer homology [PV14].

In [EPV15], they and Ellis present a decategorification of their invariant, which fits into Sartori’s picture via representations of $U_q(\mathfrak{gl}(1|1))$. It would be interesting to see how these two constructions relate to one another.

Acknowledgements. I am very grateful to my supervisor Jake Rasmussen for his constant support and for suggesting this problem to me. I would also like to thank the DPMMS for their maintenance grant for the duration of my PhD and the EPSRC for covering my fees. Furthermore, I am thankful to Vera Vértési and Ina Petkova for their talks at the ICERM workshop “Combinatorial Link Homology Theories, Braids, and Contact Geometry” in August 2014 and at the Cambridge Geometry Seminar in June 2015 and our conversations afterwards. Finally, I would like to thank Marco Marengon for his talk at our Cambridge Junior Geometry Seminars on sutured Floer homology and my “PhD brothers” for many helpful conversations.

1 The tangle invariant ∇_T^s

First of all, we define what we mean by a tangle.

Definition 1.1. Consider the closed 3-ball B^3 and a disc D^2 embedded in B^3 such that its boundary lies on ∂B^3 . (For simplicity, we may assume that D^2 is the disc obtained by intersecting ∂B^3 with a plane through the centre of B^3 .) A **tangle** is an embedding of a disjoint union of intervals and circles into B^3 such that the endpoints of the intervals lie on the boundary of D^2 . We consider tangles up to ambient isotopy fixing ∂D^2 as a set. If the number of intervals is n , we call a tangle $2n$ -ended. The images of the intervals are called open components, the images of the circles are called closed components.

A **tangle diagram** is obtained like a link diagram as the generic projection of the image of the embedding onto the disc D^2 , along with the under/over information at each singularity. Connected components of its complement in the disc are called **regions**. Those regions that meet the boundary of the disc are called **open**, the others are called **closed**. We call a diagram **connected** if the intersection of each open region with ∂D^2 is connected. **Unless specified otherwise, diagrams are assumed to be connected and have at least one crossing.** We usually do not distinguish between tangles and their diagrams unless it is clear from the context.

Example 1.2. Rational tangles are 4-ended tangles without any closed components obtained from the 4-ended tangle in figure 2a by adding twists to the top and to the right.

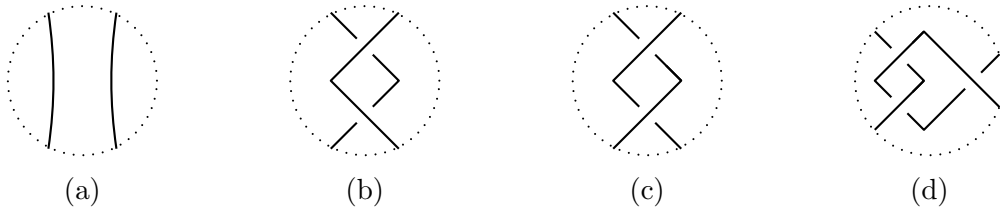


Figure 2: Some diagrams of rational tangles. (a) and (b) represent the same tangle, but only (b) is a connected diagram. (c) and (d) show some more complicated rational tangles.

Lemma 1.3. *Let T_1 and T_2 be two oriented (connected) tangle diagrams that represent the same tangle. Then there is a sequence of Reidemeister moves that connects T_1 to T_2 via connected diagrams.*

Proof. For the existence of an arbitrary sequence of Reidemeister moves from T_1 to T_2 , we refer the reader to the knot and link case. To ensure that all diagrams are connected, we can for example pick one open strand near the boundary and pull it once around the whole diagram before we go along the sequence of Reidemeister moves and undo the first step once we have arrived at T_2 . \square

Remark 1.4. One might wonder why we defined tangles the way we did. Alternatively, we could have simply allowed only those isotopies that fix the *whole* boundary sphere. However, such a definition feels too rigid, since it differentiates between far too many tangles that are essentially the same. In the other extreme, allowing just *any* isotopies would mean that we do not distinguish between tangles that are related by some twists of the tangle ends, e. g. all rational tangles would be the same, and we do not want that. The introduction of a fixed circle on the boundary sphere in definition 1.1 seems like a good compromise. It can be interpreted as a parametrisation of the punctured sphere $\partial B^3 \setminus \partial T$. We explore this point of view in section 4, see in particular proposition 4.7. It will also play an important role in section 6.

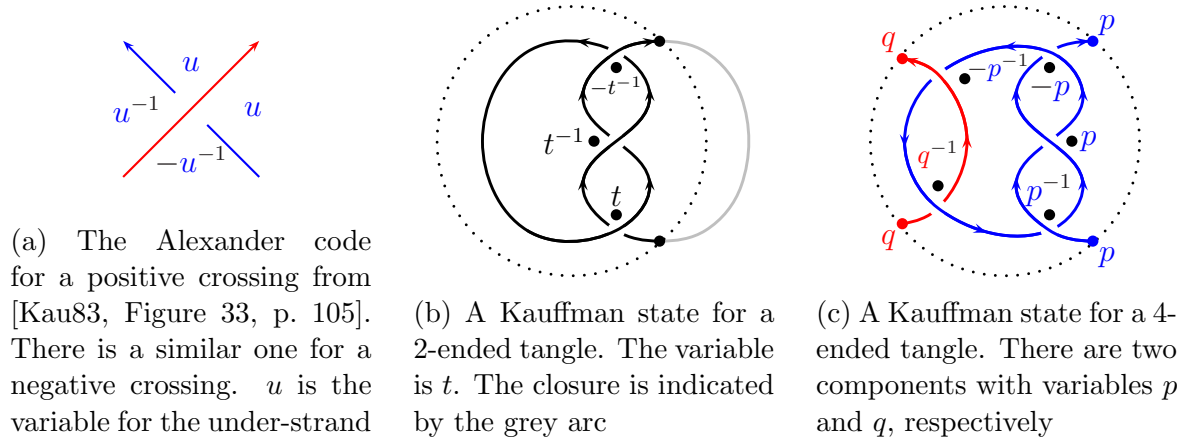


Figure 3: Applying Alexander codes to Kauffman states

Next, let us recall how the Alexander polynomial of *knots* and *links* can be computed using Kauffman states and Alexander codes. Given a diagram of a 2-ended tangle (whose closure represents a knot or link), a Kauffman state is an assignment of a marker \bullet to one of the four regions at each crossing such that each closed region is occupied by exactly one marker. One then applies the Alexander codes to the Kauffman states, i. e. one labels the markers by the monomials specified by the Alexander codes, as shown in figure 3b. To get the multivariate Alexander polynomial, one just multiplies these labels, takes the sum over all Kauffman states and finally multiplies everything by some normalisation factor.

When trying to apply this well-known algorithm to the general case of a $2n$ -ended tangle, one encounters the following problem: There are, say, m crossings in the diagram, so by an Euler characteristic argument, there are at least $(m + n + 1)$ regions. (We have

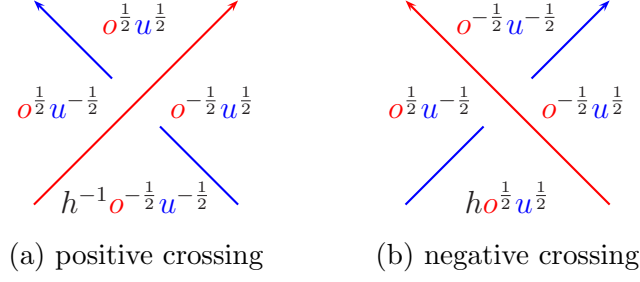


Figure 4: Alexander codes for definition 1.5. o is the variable corresponding to the over-strand and u is the variable of the under-strand.

exactly $(m + n + 1)$ regions iff all regions are simply connected. Otherwise, we have a split component and so the Alexander polynomial should be zero.) Thus, there are at least $(n + 1)$ regions more than there are markers, but the number of (pairwise distinct) open regions is $2n$. This motivates the following definition.

Definition 1.5. Let T be a (connected) diagram of an oriented $2n$ -ended tangle. A **generalised Kauffman state** of T is an assignment of a marker to one of the four regions at each crossing such that each closed region is occupied by exactly one marker, with the additional condition that there be at most one marker in each open region. A **site** of T is an $(n - 1)$ -element subsets of the set of open regions. Furthermore,

- denote the set of all generalized Kauffman states of T by $\mathbb{K} = \mathbb{K}(T)$,
- denote the set of sites by $\mathbb{S} = \mathbb{S}(T)$,
- for each $x \in \mathbb{K}$, let $s(x)$ be the set of open regions that are occupied by a marker of x , noting that $s(x)$ has $(n - 1)$ elements, so $s(x) \in \mathbb{S}$,
- for each site $s \in \mathbb{S}$, let $\mathbb{K}(T, s) := \{x \in \mathbb{K}(T) \mid s(x) = s\}$
- for each $x \in \mathbb{K}$, let $l(x)$ be the labelling of the markers of x according to the Alexander codes in figure 4,
- for each $x \in \mathbb{K}$, let $c(x)$ be the product of the labels $l(x)$.

Then for each site $s \in \mathbb{S}$, let

$$\hat{\nabla}_T^s := \sum_{x \in \mathbb{K}(T, s)} c(x).$$

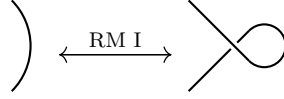
Furthermore, let ∇_T^s denote the function $\hat{\nabla}_T^s$ evaluated at $h = -1$.

Remark. The variable h stands for “homological grading”. In section 6, we define a chain complex which is generated by our generalised Kauffman states, thus generalising the hat version of knot and link Floer homology to tangles.

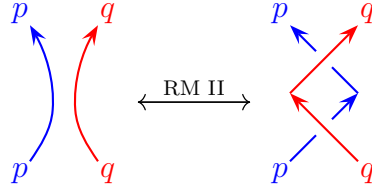
Observation 1.6. In the Alexander codes of figure 4, the exponents of u in the two regions left of an under-strand are $-\frac{1}{2}$, and $\frac{1}{2}$ in the regions on its right. For over-strands, it is the other way round. This Alexander code has the advantage over the one in figure 3a that we do not need to multiply ∇_T^s by a normalisation factor to make it into a tangle invariant.

Theorem 1.7. *For two oriented tangle diagrams T_1 and T_2 representing the same tangle and $s \in \mathbb{S}(T_1) = \mathbb{S}(T_2)$, we have $\nabla_{T_1}^s = \nabla_{T_2}^s$. So ∇ is a tangle invariant.*

Proof. By lemma 1.3, we just need to check that the polynomials are invariant under the Reidemeister moves RM I–III. We can check this locally, so the proof becomes exactly the same as for the usual knot and link case. We only check RM I and II here; for a complete proof, we refer the reader to the Mathematica notebook [nb] which contains a program to calculate ∇_T^s for any connected tangle diagram T and site s . RM I looks as follows:



The enclosed region only has one crossing, so the corresponding marker has to sit in that region in every Kauffman state. Then, for both orientations, the labelling of this marker is 1. The same holds if we reverse the crossing; we can either check this directly, or apply proposition 2.1. For RM II, we only check one orientation; again, for the others, we can either check this separately or simply apply proposition 2.4.



In the diagram on the right, there are exactly two Kauffman states that occupy the open region on the left; they contribute p^{-1} and $h^{-1}p^{-1}$, so after setting $h = -1$, they cancel. The same is true for the open region on the right; the contribution there is q^{-1} and $h^{-1}q^{-1}$. Finally, for each of the open regions at the top and the bottom, there is exactly one Kauffman state and it contributes 1. \square

We have chosen the letter ∇ for a reason:

Theorem 1.8. *Let T be a diagram of an oriented 2-ended tangle representing a link or knot L . Note that in this case there is only one site of T , namely the empty set \emptyset . Let the variable corresponding to the open component be c . Then*

$$\frac{1}{c - c^{-1}} \nabla_T^\emptyset$$

is equal to the Conway potential function ∇_L .

Proof. Verify that $\nabla := \frac{1}{c - c^{-1}} \nabla_T^\emptyset$ satisfies the axioms in [Jia14], see [nb]. \square

Remark 1.9. Recall that the Conway potential function of an n -component oriented link L is a rational function $\nabla_L(t_1, \dots, t_n)$ which is related to the multivariate Alexander polynomial Δ_L in the following way: (see for example [Har83] or [Jia14])

$$\nabla_L(t_1, \dots, t_n) = \begin{cases} \frac{\Delta_L(t^2)}{t - t^{-1}}, & \text{if } n = 1; \\ \Delta_L(t_1^2, \dots, t_n^2), & \text{if } n > 1. \end{cases}$$

Hence, using the notation of the theorem above

$$\nabla_T^\emptyset(t_1, \dots, t_n) = \begin{cases} \Delta_L(t^2), & \text{if } n = 1; \\ (c - c^{-1})\Delta_L(t_1^2, \dots, t_n^2), & \text{if } n > 1. \end{cases}$$

We also note that ∇_T^\emptyset of a 2-ended tangle T , multiplied by a factor of $(c - c^{-1})$ for each *closed* component of T , is equal to the Euler characteristic of \widehat{HFL} as defined in [OS07].

We collect some properties of the Conway potential function in the following theorem.

Theorem 1.10. *The Conway potential function of an oriented link L satisfies the following properties:*

(i) *If $m(L)$ denotes the mirror image of L , then*

$$\nabla_{m(L)}(t_1, \dots, t_r) = (-1)^{r-1} \cdot \nabla_L(t_1, \dots, t_r).$$

(ii) $\nabla_L(t_1, \dots, t_r) = (-1)^r \cdot \nabla_L(t_1^{-1}, \dots, t_r^{-1})$.

(iii) *If $r(L, t_1)$ is obtained from L by reversing the orientation of the first strand, then*

$$\nabla_{r(L, t_1)}(t_1, \dots, t_r) = -\nabla_L(t_1^{-1}, t_2, \dots, t_r).$$

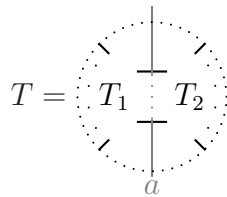
(iv) *If L_1, \dots, L_r denote the link components of L , then*

$$\nabla_L(1, t_2, \dots, t_r) = (t_2^{\text{lk}(L_1, L_2)} \dots t_r^{\text{lk}(L_1, L_r)} - t_2^{-\text{lk}(L_1, L_2)} \dots t_r^{-\text{lk}(L_1, L_r)}) \nabla_{L \setminus L_1}(t_2, \dots, t_r).$$

Proof. See propositions 5.6, 5.5, 5.7 and 5.3 in [Har83]. □

Often, we want to glue tangle diagrams together along some of their boundary to obtain new tangle diagram. We can easily compute the polynomial invariant of the new tangle from the invariants of the two glued components. (In fact, we have implicitly used the fact that ∇_T^s behaves well under glueing in the proof of theorem 1.7 already.) Note that the following result generalises the connected sum formula for knots and links.

Proposition 1.11 (splitting/gluing formula). *Let T_1 and T_2 be two oriented tangles obtained by splitting an oriented tangle diagram T along some arc a that does not meet any crossings:*



Let $t_{1,1}, \dots, t_{1,r_1}, t_{2,1}, \dots, t_{2,r_2}$ and t_1, \dots, t_r be the variables corresponding to the components in T_1, T_2 and T , respectively. Gluing T_1 and T_2 back together induces an identification of these variables which gives rise to two homomorphisms

$$\iota_i : \mathbb{Z}[t_{i,1}^{\pm 1/2}, \dots, t_{i,r_i}^{\pm 1/2}] \rightarrow \mathbb{Z}[t_1^{\pm 1/2}, \dots, t_r^{\pm 1/2}], \quad i = 1, 2.$$

Then

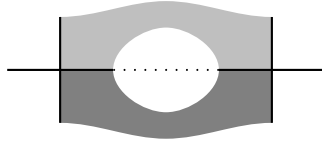
$$\hat{\nabla}_T^s = \sum_{\substack{s_1 \cap s_2 = \emptyset \\ (s_1 \cup s_2) \cap O(T) = s}} \iota_1(\hat{\nabla}_{T_1}^{s_1}) \cdot \iota_2(\hat{\nabla}_{T_2}^{s_2}),$$

where $O(T)$ denotes the set of open regions in the diagram T .

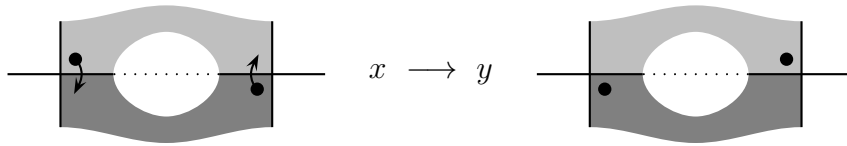
Proof. This follows immediately from definition 1.5. □

Before moving on to the next section to study some properties of our tangle invariant, we state a generalisation of Kauffman's clock theorem [Kau83, Theorem 2.5] to tangles. For this we recall the following definition from [Kau83, p. 18]. (Note that the theorem is false if we use the stronger definition given in the introduction of the same monograph¹.)

Definition 1.12. Suppose in a tangle diagram, there are two crossings which have two regions in common as illustrated below.



Suppose further that in a Kauffman state x , the markers of the two crossings lie in these two regions. Then there also exists a Kauffman state y obtained from x by moving each of the markers of the two crossings in exactly the opposite region. We say that we go from x to y by a **transposition move**. A transposition move is called **clockwise** if the markers move clockwise around each crossing:



The reverse is called a **counterclockwise** move.

Theorem 1.13 (generalised clock theorem). *Let T be a (not necessarily connected) tangle diagram and $s \in \mathbb{S}(T)$. Then $\mathbb{K}(T, s)$ is a finite lattice under the relation*

$$x > y \Leftrightarrow \exists \text{ sequence of clockwise transposition move from } x \text{ to } y.$$

Proof. See the appendix. □

¹Many thanks to Tom Brown for pointing out this trap to me that I had wandered into.

2 Some basic properties of ∇_T^s

In this section, we collect and prove some properties of the tangle invariants ∇_T^s , guided by theorem 1.10. We will see that with the exception of the symmetry property (ii), the results generalise to the tangle case. Our generalisation of property (iv) leaves room for improvement because it only applies to closed components. For open components, some better understanding of the relations between sites would probably be helpful.

The first proposition below corresponds to part (i) combined with (ii) of theorem 1.10.

Proposition 2.1. *Let T be an oriented tangle and $m(T)$ its mirror image. Then for all $s \in \mathbb{S}(T)$,*

$$\hat{\nabla}_{m(T)}^s(t_1, \dots, t_r, h) = \hat{\nabla}_T^s(t_1^{-1}, \dots, t_r^{-1}, h^{-1}).$$

Proof. Observe that the two Alexander codes in figure 4 are mirror images of one another after taking the reciprocals of all variables. \square

Definition 2.2. We define the **linking number** $\text{lk}_T(p, q)$ for two components p and q of a tangle T to be

$$\text{lk}_T(p, q) := \frac{1}{2}(\#\{\text{positive crossings of } p \text{ and } q\} - \#\{\text{negative crossings of } p \text{ and } q\}).$$

For a tangle with a component t_j , we also define

$$\text{lk}_T(t_j) := \sum \text{lk}_T(t_i, t_j),$$

where the sum is over all components $t_i \neq t_j$. We sometimes omit the subscript when there is no risk of ambiguity.

Remark. Note that for two-component links, $\text{lk}(p, q)$ coincides with the usual linking number. Also, linking numbers are invariants of tangles.

The generalised clock theorem implies the following basic property.

Corollary 2.3. *Given a tangle diagram T , the powers of any variable in two Kauffman states of the same site $s \in \mathbb{S}(T)$ differ by a multiple of 2. Furthermore, the exponent of a variable p in $\hat{\nabla}_T^s$ is an integer iff $\text{lk}(p)$ is an integer.*

Proof. By the generalised clock theorem (theorem 1.13), any two Kauffman states with site s are connected by a sequence of transposition moves. It is easy to see that two states connected by a single transposition move have either the same Alexander grading or the exponents of one variable (the one corresponding to the horizontal strand) changes by ± 2 .

The second statement follows directly from the definition of the linking number. \square

The next proposition corresponds to part (iii) of theorem 1.10.

Proposition 2.4. *Let T be an oriented r -component tangle. If $r(T, t_1)$ denotes the same tangle T with the orientation of the first strand reversed, then for all sites $s \in \mathbb{S}(T)$, we have*

$$\hat{\nabla}_{r(T, t_1)}^s(t_1, \dots, t_r) = h^{\text{lk}_T(t_1)} \hat{\nabla}_T^s(h^{-1}t_1^{-1}, t_2, \dots, t_r).$$

Proof. This is easily seen by considering crossings separately: Modulo sign, the statement follows from observation 1.6. For the correct sign, note that after substituting $h^{-1}t_1^{-1}$ into the Alexander code of a positive (negative) crossing involving t_1 and some different variable, we obtain the Alexander code of the crossing with the orientation of the t_1 -strand reversed multiplied by $h^{-\frac{1}{2}}$ (respectively $h^{\frac{1}{2}}$). For crossings involving only t_1 , no additional factor is necessary, and for crossings not involving t_1 at all, there is nothing to show. \square

Note that one has to be careful when setting $h = -1$ in the proposition above, because the $\hat{\nabla}_T^s$ are Laurent polynomials with half-integer powers. The same applies to corollary 2.5 below. In corollary 2.12, we give a formula that is more convenient when working with ∇_T^s instead of $\hat{\nabla}_T^s$.

Corollary 2.5. *Let T be an oriented r -component tangle. If $r(T)$ denotes the same tangle T with the orientation of all strands reversed, then for all sites $s \in \mathbb{S}(T)$, we have*

$$\hat{\nabla}_{r(T)}^s(t_1, \dots, t_r) = \hat{\nabla}_T^s(h^{-1}t_1^{-1}, \dots, h^{-1}t_r^{-1}).$$

Proof. We successively reverse the orientation of all strands, noting that each term $\text{lk}_T(t_i, t_j)$ appears twice in the exponent of h , but with different signs, because the second time it appears, the orientation of one strand has been reversed. \square

Corollary 2.6. *Let $r(\cdot)$ denote the function which substitutes $-t^{-1}$ for each variable t . Then, for an oriented link L , we have the symmetry relation*

$$\nabla_L = \nabla_{r(L)} = r(\nabla_L).$$

Proof. The first equality is theorem 1.10 (ii) and (iii), the second follows from theorem 1.8 and the corollary above with $h = -1$. \square

Lemma 2.7 (one-colour skein relation). *Let L_+ , L_- and L_o denote the tangles \nearrow, \nwarrow and \searrow respectively. Then for all sites s ,*

$$\nabla_{L_+}^s(t, t) - \nabla_{L_-}^s(t, t) = (t - t^{-1}) \cdot \nabla_{L_o}^s(t, t). \quad \square$$

Corollary 2.8. *Let T be a 2-ended tangle representing a knot. Then $\nabla_T^s(\pm 1) = 1$.*

Proof. Let T' be the diagram obtained from T by changing some crossings such that T' represents the unknot. Then by the lemma above, $\nabla_T^s(\pm 1) = \nabla_{T'}^s(\pm 1)$, and $\nabla_{T'}^s(t) \equiv 1$. \square

Corollary 2.9. *The one-variable polynomial tangle invariant $\nabla_T^s(t, \dots, t)$ satisfies the same skein relation as the Alexander polynomial.*

Proof. This follows from lemma 2.7 using a glueing argument similar to proposition 1.11. \square

The next proposition corresponds to part (iv) of theorem 1.10.

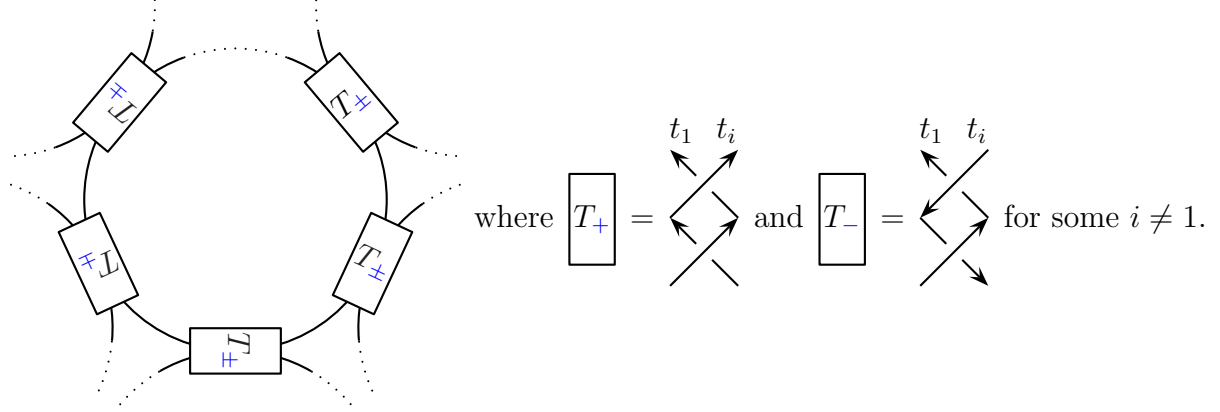
Proposition 2.10. *Let T be a tangle with a closed component K_1 . Then for all sites $s \in \mathbb{S}$, $\nabla_T^s(\pm 1, t_2, \dots, t_r)$ is equal to*

$$(\pm 1)^{\text{lk}(t_1)+1} (t_2^{\text{lk}(t_1, t_2)} \dots t_r^{\text{lk}(t_1, t_r)} - t_2^{-\text{lk}(t_1, t_2)} \dots t_r^{-\text{lk}(t_1, t_r)}) \cdot \nabla_{T \setminus K_1}^s(t_2, \dots, t_r).$$

Proof. First we apply lemma 2.7 to t_1 - t_1 -crossings in T . Setting $t_1 = \pm 1$ gives

$$\nabla_T^s(\pm 1, t_2, \dots, t_r) = \nabla_{T'}^s(\pm 1, t_2, \dots, t_r),$$

where T' denotes the tangle obtained by swapping over- and under-strands at some t_1 - t_1 -crossing. We can therefore assume wlog that the t_1 -component is the unknot, in particular that there are no t_1 - t_1 -crossings and near the t_1 -component, the diagram looks as follows:



The following table gives the values of $\nabla_{T_\pm}^s$, where l, b, r, t denote the regions on the left, bottom, right and top of the diagrams T_\pm , respectively.

s	T_+	T_-		s	T_+	T_-
l	$(t_i - t_i^{-1})$	$-(t_i - t_i^{-1})$	so after setting $t_1 = \pm 1$:	l	$(t_i - t_i^{-1})$	$-(t_i - t_i^{-1})$
b	$t_1^{-1} t_i^{-1}$	$t_1^{-1} t_i$		b	$\pm t_i^{-1}$	$\pm t_i$
r	$(t_1 - t_1^{-1})$	$-(t_1 - t_1^{-1})$		r	0	0
t	$t_1 t_i$	$t_1 t_i^{-1}$		t	$\pm t_i$	$\pm t_i^{-1}$

Let the number of rectangular boxes T_\pm be denoted by n . The fact that $\nabla_{T_\pm}^r(1, t_i) = 0$ means that if we consider the picture above as a $2n$ -ended tangle T'' , there are at most n sites such that the polynomial invariant becomes non-zero after substituting $t_1 = \pm 1$. Each of these sites is specified by the region which is not occupied by a marker and which is not a right region of any box T_\pm . Fix such a region u . Then each Kauffman state of T'' is determined by a box and a marker in the left region of this box. For each box, there are two such Kauffman states, namely those that contribute to ∇^l of that box.

We introduce the following notation: We number the boxes in counter-clockwise direction, starting from the fixed unoccupied region u . Let $\alpha_j^{i\pm}$ denote the number of T_\pm s involving the i^{th} strand in counter-clockwise direction from u to the j^{th} box T_j . Similarly, let $\beta_j^{i\pm}$ denote the number of T_\pm s involving the i^{th} strand in clockwise direction from u to T_j . Let $i_j \neq 1$ denote the index of the strand involved in T_j . The contribution of the boxes $T_\pm \neq T_j$ to the labelling of the two Kauffman states corresponding to T_j is

$$\begin{aligned} \alpha_j^{i+} &\rightarrow \pm t_i, \\ \alpha_j^{i-} &\rightarrow \pm t_i^{-1}, \\ \beta_j^{i+} &\rightarrow \pm t_i^{-1}, \\ \beta_j^{i-} &\rightarrow \pm t_i, \end{aligned}$$

so that the contribution of the two Kauffman states to $\nabla_{T''}$ of the site determined by u is

$$\pm(t_{i_j} - t_{i_j}^{-1}) \cdot \prod_{i \neq 1} (\pm t_i)^{(\alpha_j^{i+} + \beta_j^{i-}) - (\alpha_j^{i-} + \beta_j^{i+})}.$$

Note that by definition

$$\text{lk}(t_1, t_i) = \begin{cases} \alpha_j^{i+} - \alpha_j^{i-} + \beta_j^{i+} - \beta_j^{i-} & \text{if } i \neq 1, i_j, \\ \alpha_j^{i+} - \alpha_j^{i-} + \beta_j^{i+} - \beta_j^{i-} + 1 & \text{if } i = i_j \text{ and } T_j = T_+, \\ \alpha_j^{i+} - \alpha_j^{i-} + \beta_j^{i+} - \beta_j^{i-} - 1 & \text{if } i = i_j \text{ and } T_j = T_-. \end{cases}$$

So the expression above becomes

$$\begin{aligned} & \pm(t_{i_j} - t_{i_j}^{-1}) \cdot (\pm t_{i_j})^{\text{lk}(t_1, t_{i_j}) - 2(\beta_j^{i_j+} - \beta_j^{i_j-}) \mp 1} \cdot \prod_{i \neq 1, i_j} (\pm t_i)^{\text{lk}(t_1, t_i) - 2(\beta_j^{i+} - \beta_j^{i-})} = \\ & \pm \left((\pm t_{i_j})^{\text{lk}(t_1, t_{i_j}) - 2(\beta_j^{i_j+} - \beta_j^{i_j-})} - (\pm t_{i_j})^{\text{lk}(t_1, t_{i_j}) - 2(\beta_j^{i_j+} - \beta_j^{i_j-}) \pm 1} \right) \cdot \prod_{i \neq 1, i_j} (\pm t_i)^{\text{lk}(t_1, t_i) - 2(\beta_j^{i+} - \beta_j^{i-})}. \end{aligned}$$

Now, consider two consecutive boxes, say the j^{th} and the $(j+1)^{\text{st}}$ box. Then

$$\beta_j^{i_j+} - \beta_j^{i_j-} = \beta_{j+1}^{i_j+} - \beta_{j+1}^{i_j-} \pm 1.$$

and for all other variables, the exponents remain the same. So we see that most terms cancel and the only surviving ones are the second one of the first box and the first one of the last box. But

$$\beta_1^{i_1+} - \beta_1^{i_1-} = \begin{cases} \text{lk}(t_1, t_i) & \text{if } i \neq 1, i_1, \\ \text{lk}(t_1, t_{i_1}) \mp 1 & \text{if } i = i_1, \end{cases}$$

and

$$\beta_n^{i_n+} = \beta_n^{i_n-} = 0 \quad \text{for all } i \neq 1,$$

so we are done. \square

Proposition 2.11. *Given a tangle T , we can compute the powers modulo 2 appearing in the labellings of Kauffman states as follows. If the variable t corresponds to a closed component in T , its exponents are equal to $\text{lk}(t) + 1 \pmod{2}$. If the variable t corresponds to an open component, its exponents are equal to*

$$\text{lk}(t) + 1 + \frac{1}{2}(s_i - s_o + r_o - r_u - 1) \equiv \text{lk}(t) + 1 + s_i + r_u \pmod{2},$$

where, if we follow the outgoing t -strand in counter-clockwise direction along the boundary of the disc to the other end, s_i is the number of ingoing strands, s_o is the number of outgoing strands, r_o is the number of occupied regions and r_u is the number of unoccupied regions that we meet along the way.

Remark. It is easy to see that the formula is symmetric in the sense that it does not matter if we go clock- or counter-clockwise. Nonetheless, it would be nice to find a more natural interpretation of this formula. Again, a better understanding of the relations between site would probably be useful for this.

Corollary 2.12 (reversing orientations revisited). *Let T be an oriented r -component tangle. If $r(T, t_1)$ denotes the same tangle T with the orientation of the first component K_1 reversed, then for all sites $s \in \mathbb{S}(T)$, we have*

$$\nabla_{r(T, t_1)}^s(t_1, \dots, t_r) = \begin{cases} -\nabla_T^s(t_1^{-1}, t_2, \dots, t_r) & K_1 \text{ is a closed component,} \\ (-1)^{2\text{lk}_T(t_1)+1+s_i+r_u} \nabla_T^s(t_1^{-1}, t_2, \dots, t_r) & K_1 \text{ is an open component,} \end{cases}$$

where we use the same notation as in the previous proposition. Similarly, if $r(T)$ denotes the same tangle T with the orientation of all strands reversed, then for all sites $s \in \mathbb{S}(T)$, we have

$$\nabla_{r(T)}^s(t_1, \dots, t_r) = (-1)^{r+c+\sum s_i+\sum r_u} \nabla_T^s(t_1^{-1}, \dots, t_r^{-1}),$$

where $c \equiv \sum \text{lk}(t_i) \pmod{2}$ is the number of interlinked pairs of endpoints of the same colour on the boundary of the disc.

Proof. The first part follows directly from proposition 2.4 and 2.11. For the second part, we apply proposition 2.11 to corollary 2.5. \square

Before we come to the proof of proposition 2.11, we do some preparation first.

Lemma 2.13. *Let T be a tangle with no closed components. Then there exists a site $s \in \mathbb{S}(T)$ such that $\nabla_T^s \neq 0$.*

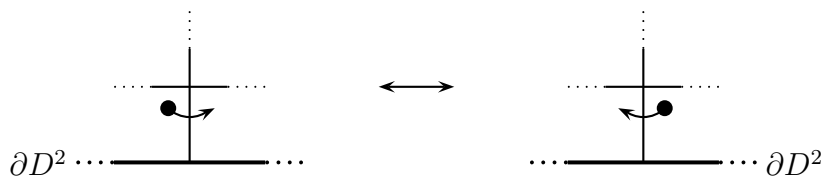
Proof. We extend the diagram T to one of a knot by successively connecting two ends of strands with different orientations and colours until only two ends are left. (Note that this process might introduce some more crossings.) Then ∇^s of this knot will be a linear combination of the ∇_T^s . Since it is also non-zero (say, by corollary 2.8), ∇_T^s cannot be identically zero for all s . \square

Lemma 2.14. *Let T be a (connected) tangle diagram (with at least one crossing). Then there exists a site s such that $\mathbb{K}(T, s)$ is non-empty.*

Proof. As in the previous proof, we close all but two strands of the diagram in some fashion. This new diagram represents a link and, by [Kau83, lemma 2.2, theorem 2.4], it has a Kauffman state. Hence its restriction to the original tangle diagram is also a Kauffman state for some site s . \square

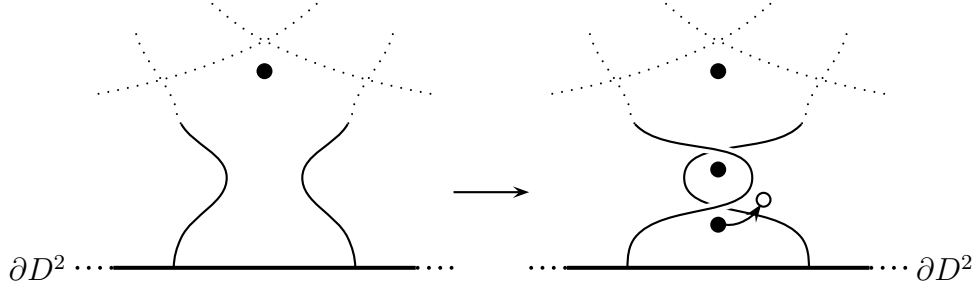
Lemma 2.15. *Given a tangle T , let x and x' be two Kauffman states whose sites s and s' differ in exactly two adjacent open regions, separated by the strand corresponding to the variable t . Then the exponent of t in the labelling of x and x' differs by 1 modulo 2. Exponents of other variables agree modulo 2.*

Proof. As in the proof of Corollary 2.3, we would like to have some simple move that we can perform to get from one site to another and that affects the labels in a predictable way and then appeal to some connectedness result. Here, the basic move is the following, we call it the boundary move:



Consider two Kauffman states which are related by a single boundary move. The labellings of these two Kauffman states differ by the factor $t^{\pm 1}$.

However, such a boundary move might not always be possible. To fix this, we first modify the diagram slightly, namely we perform a Reidemeister II move as follows:



The labelling of the new Kauffman state corresponding to x as shown in the right picture above is the same as the labelling of x itself. The same is true for the labelling of x' . (The additional two markers are then on the “top” of the new crossings.) We can now perform a boundary move as indicated by the arrow in the picture on the right. By corollary 2.3, the powers of each variable in the labellings of this Kauffman state and x' agree modulo 2. \square

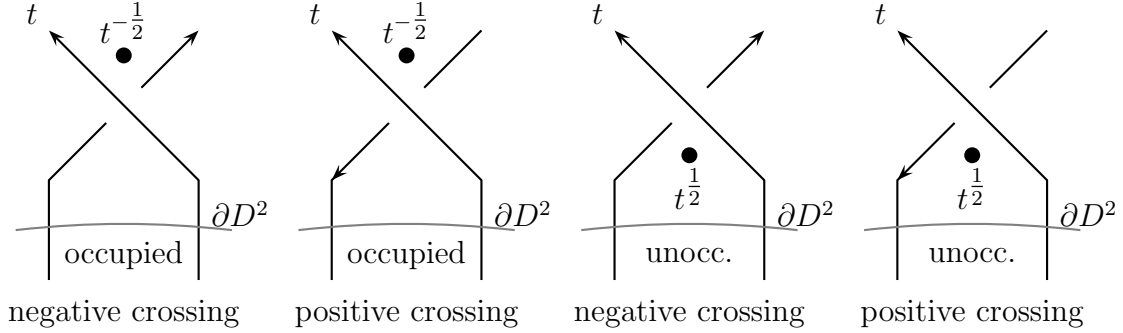
Lemma 2.16. *For any (not necessarily connected) tangle diagram T , we can find an equivalent diagram T' such that for any site $s \in \mathbb{S}(T) = \mathbb{S}(T')$, T' has a Kauffman state. Furthermore, the labelling of any Kauffman state of T agrees with the labelling of any Kauffman state in T' belonging to the same site, considering any exponents modulo 2.*

Proof. If there is no Kauffman state in T , we can modify the diagram such that the hypotheses of lemma 2.14 are satisfied. So we may assume without loss of generality that there exists a Kauffman state in T for some site. We now repeatedly apply the same method as in the proof above, noting that a Reidemeister II move merely enlarges the set of Kauffman states and the labellings of corresponding Kauffman states agree. \square

Proof of proposition 2.11. Let s be the site of a Kauffman state x . We consider closed components first. Suppose that all linking numbers are non-zero. Then the claim follows from proposition 2.10 and corollary 2.3 if ∇^s of the tangle T with all closed components removed is not identically zero. By lemma 2.13, we can find at least one site s' of this tangle, such that for any Kauffman state in $\mathbb{K}(T, s')$, the claim is true. By lemma 2.16, we may assume that there is a Kauffman state for each site. Then by lemma 2.15, we know that in particular the exponents of the variables corresponding to closed components agree for all sites.

The general case, where linking numbers may be zero, can be reduced to the first case. For this, we modify the diagram as follows: Consider two strands whose mutual linking number is zero. If they meet at a crossing, we can reverse the over- and under-strands at one such crossing. This changes both the linking number and the exponents of both variables by ± 1 . If two components have no crossing in common, we perform some Reidemeister II moves to pull one strand across the other to get one. Note that this does not affect the labelling of the Kauffman states (as in the previous proof). This finishes the proof for closed components.

For open components, the idea is to add twists at the outgoing strand until it bounds the same open region as the incoming strand, so that for some sites, we can close this component and apply the result above. We use the convention that the t -strand always goes over its left neighbour. We can then distinguish the following cases, depending on the orientation of the other strand involved and on whether the open region between these two strands is occupied by a marker or not:



Now, suppose the open region on the left of the incoming t -strand is occupied. Then we can close the t -component and apply the result above. The exponent of t in the original diagram is equal to $\text{lk}_{\text{new}}(t) + 1 + \frac{1}{2}((r_o - 1) - r_u)$, where $\text{lk}_{\text{new}}(t)$ denotes the linking number of the closed t -component in the new diagram. Suppose the open region on the left of the incoming t -strand is unoccupied, so we cannot close the t -component. One way to solve this problem is by “pushing” a marker of an open region into this region, using lemmas 2.16 and 2.15. However, this does not work for 2-ended tangles where we do not have any markers to “push around”. Although one can, of course, look at this case separately, we give an alternative argument that works in general: We still close the t -component, but instead of gluing a single strand to the diagram, we attach a diagram that consists of two parallel strands that are twisted by a Reidemeister II move. By considering ∇ for the attached two-crossing diagram, we see that the exponent of t in the original Kauffman state is given by $\text{lk}_{\text{new}}(t) + 1 + \frac{1}{2}(r_o - (r_u - 1)) + 1 \pmod{2}$, i.e. the same formula as in the first case.

So it remains to calculate $\text{lk}_{\text{new}}(t)$. We have $\text{lk}_{\text{new}}(t) = \text{lk}_T(t) + \frac{1}{2}(s_i - s_o)$. Substituting this into the formula above gives the first formula in the statement of the proposition. The equivalence to the second one is seen by substituting the obvious identity $s_i + s_o = r_o + r_u - 1$ into the first formula (and adding $2r_u$). \square

3 4-ended tangles and mutation invariance

Proposition 3.1. *Let T be a 4-ended tangle. Then the endpoints of the same strands are either neighbours on ∂D^2 (case I) or not (case II). We consider the following orientations for these two cases:*



Then in both cases,

$$\nabla_T^b = \nabla_{r(T)}^d. \quad (\text{b-d})$$

Furthermore, in case I

$$(p - p^{-1}) \cdot \nabla_T^a = (q - q^{-1}) \cdot \nabla_T^c, \quad (\text{I a-c})$$

$$\nabla_T^c = \nabla_{r(T)}^c \text{ and} \quad (\text{I c-c})$$

$$(pq - p^{-1}q^{-1}) \cdot \nabla_T^c = (p - p^{-1}) (\nabla_T^d - \nabla_{r(T)}^d) \quad (\text{I c-d})$$

and in case II

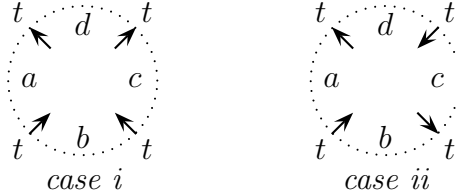
$$\nabla_T^a = \nabla_{r(T)}^c, \quad (\text{II a-c})$$

$$(pq - p^{-1}q^{-1}) \cdot \nabla_T^c = (p - p^{-1}) \cdot \nabla_T^d - (q - q^{-1}) \cdot \nabla_{r(T)}^d \text{ and} \quad (\text{II c-d})$$

$$(p^{-1}q - pq^{-1}) \cdot \nabla_T^d = (q - q^{-1}) \cdot \nabla_T^a - (p - p^{-1}) \cdot \nabla_{r(T)}^a. \quad (\text{II d-a})$$

For orientations different from the above, we get similar relations, which we can easily compute using proposition 2.4 and 2.11.

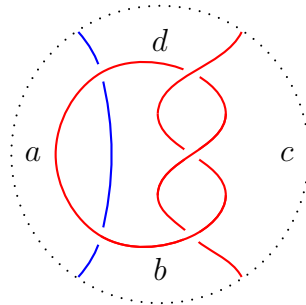
Corollary 3.2. *Let T be a 4-ended tangle. We distinguish between the following two cases:*



We write $a = \nabla_T^a(t, t, t_1, \dots, t_{r-2})$, $a_{rev} = \nabla_{r(T)}^a(t, t, t_1, \dots, t_{r-2})$ and similarly for b, c and d . Then in both cases, we have $c = a = a_{rev}$ and $b = d_{rev}$. In case ii, we additionally get $b = d$.

Proof. The first identity is seen by closing a or c . The second follows from the properties of the Conway potential function, theorem 1.10(ii) and (iii). The third follows from proposition 3.1. The fourth relation is seen again by closing b or d . \square

Remark. Proposition 3.1 tells us that there is basically only one piece of information in the polynomial Alexander invariant of 4-ended tangles. One might ask whether all four invariants in case I contain the same information like in case II. However, this is not the case: For any knot K , we can consider the two-component tangle diagram obtained from K by cutting it once to get one strand of the tangle, adding an unknotted strand to it and performing a Reidemeister II move to get rid of any multiple regions on the boundary, like in the following example for $K = \text{trefoil knot}$:

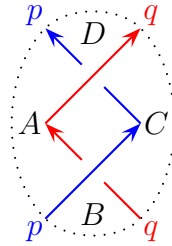


Then both a and c are zero because closing either of these regions results in a link diagram with two unlinked components. However, for matching orientations of the strands, b and d both give the Alexanderpolynomial Δ_K of the knot K .

Proof. Relation (I a-c) follows from theorem 1.8 and the fact that the two diagrams obtained by closing either the p -component or the q -component both represent the same link. Next, using the notation from corollary 2.6 and the corollary itself, we obtain

$$r\left(\frac{\nabla_T^c}{p - p^{-1}}\right) = \frac{\nabla_T^c}{p - p^{-1}}.$$

so we immediately get (I c-c). Next, we compute the invariants for the following tangle U :



$$\begin{aligned} A &:= \nabla_U^A = (q - q^{-1}) \\ B &:= \nabla_U^B = p^{-1}q^{-1} \\ C &:= \nabla_U^C = (p - p^{-1}) \\ D &:= \nabla_U^D = pq \end{aligned}$$

We observe that the diagrams obtained by gluing the above diagram either to the top or to the bottom of T and closing the q -component represent the same link. In the first case, the corresponding polynomial is given by $C \cdot \nabla_T^d + B \cdot \nabla_T^c$ and the second, by $C \cdot \nabla_T^b + D \cdot \nabla_T^c$. Again, corollary 2.6 implies

$$r\left(\frac{C \nabla_T^d + B \nabla_T^c}{p - p^{-1}}\right) = \frac{C \nabla_T^d + B \nabla_T^c}{p - p^{-1}} = \frac{C \nabla_T^b + D \nabla_T^c}{p - p^{-1}}, \quad (1)$$

After some simplification, we get

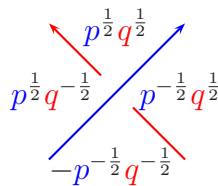
$$r(C) \cdot \nabla_{r(T)}^d + r(B) \cdot \nabla_{r(T)}^c = C \cdot \nabla_T^b + D \cdot \nabla_T^c$$

Finally, using $r(B) = D$ and $r(C) = C$, we obtain the desired identities (b-d) for case I. For (I c-d), we just use the first half of equations (1) and, after simplification, we get

$$r(C) \cdot \nabla_{r(T)}^d + r(B) \cdot \nabla_{r(T)}^c = C \cdot \nabla_T^d + B \cdot \nabla_T^c.$$

Substituting $\nabla_{r(T)}^c$, $r(B)$ and $r(C)$ gives the desired identity.

By a similar method, we can derive the relations for case II. We first show the second relation. For this, we apply the corresponding statement from case I to the diagram obtained by gluing a positive twist to the bottom of T .



Then, we have

$$-p^{-\frac{1}{2}}q^{-\frac{1}{2}}\nabla_T^b = r\left(p^{\frac{1}{2}}q^{\frac{1}{2}}\nabla_T^d\right),$$

which is (b-d). (II c-d) follows similarly; we have

$$(pq - p^{-1}q^{-1}) \cdot \left(p^{\frac{1}{2}}q^{\frac{1}{2}}\nabla_T^c + p^{-\frac{1}{2}}q^{\frac{1}{2}}\nabla_T^b\right) = (p - p^{-1}) \left(p^{\frac{1}{2}}q^{\frac{1}{2}}\nabla_T^d - r\left(p^{\frac{1}{2}}q^{\frac{1}{2}}\nabla_T^d\right)\right).$$

Substituting ∇_T^b yields

$$\begin{aligned} (pq - p^{-1}q^{-1})\nabla_T^c &= (p - p^{-1})\nabla_T^d + (q^{-1} - p^{-2}q^{-1}) \cdot \nabla_{r(T)}^d - (q - p^{-2}q^{-1}) \cdot \nabla_{r(T)}^d \\ &= (p - p^{-1})\nabla_T^d - (q - q^{-1})\nabla_{r(T)}^d. \end{aligned}$$

For (II a-c), we compare the two diagrams obtained by gluing a single positive twist either to the top or to the bottom of T and closing the q -strand. We obtain

$$r\left(\frac{-p^{-\frac{1}{2}}q^{-\frac{1}{2}}\nabla_T^a + p^{\frac{1}{2}}q^{-\frac{1}{2}}\nabla_T^d}{p - p^{-1}}\right) = \frac{p^{\frac{1}{2}}q^{\frac{1}{2}}\nabla_T^c + p^{-\frac{1}{2}}q^{\frac{1}{2}}\nabla_T^b}{p - p^{-1}},$$

This simplifies to

$$p^{\frac{1}{2}}q^{\frac{1}{2}}\nabla_{r(T)}^a + p^{-\frac{1}{2}}q^{\frac{1}{2}}\nabla_{r(T)}^d = p^{\frac{1}{2}}q^{\frac{1}{2}}\nabla_T^c + p^{-\frac{1}{2}}q^{\frac{1}{2}}\nabla_T^b$$

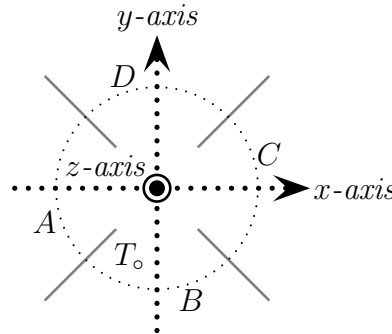
Using (b-d), the result follows. Finally, relation (II d-a) is obtained from the previous one using proposition 2.4 and 2.11. We reverse the p -strand, so we get

$$(pq^{-1} - p^{-1}q) \cdot \nabla_{r(T,p)}^c = (p - p^{-1}) \cdot \nabla_{r(T,p)}^d - (q - q^{-1}) \cdot \nabla_{r(r(T),p)}^d.$$

We observe that $r(T, p)$ also belongs to case II; however, to get the same configuration as in the proposition, we have to rotate it by 90° counter-clockwise and switch p and q . Doing this for the identity above gives us the required result. \square

Next, we see that the polynomials are invariant under mutation.

Theorem 3.3 (mutation invariance). *Let T be an oriented tangle and T_\circ a 4-ended tangle obtained by intersecting a closed 3-ball with T such that the two open components of T_\circ belong to the same component in T (or their variables are set equal to one another). Let T' be the oriented tangle obtained from T by mutation at T_\circ , i. e. rotation of T_\circ by π about one of the three axes below.*

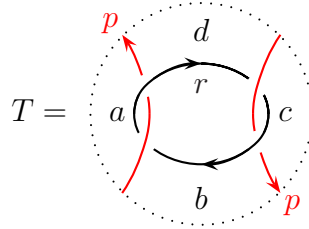


If the orientation of the two open components of T_\circ needs to be reversed for this, we also reverse the orientation of all other components of T_\circ in T' ; otherwise we do not change any orientations. Then for all sites $s \in \mathbb{S}(T) = \mathbb{S}(T')$,

$$\nabla_T^s = \nabla_{T'}^s.$$

Corollary 3.4. *The multivariable Alexander polynomial is mutation invariant, provided that the open strands of the mutating tangle have the same colour and that if the mutation changes the orientation of those open strands, we also change the orientation of all closed strands in the mutating tangle.* \square

Remark 3.5. It is quite easy to find a counterexample for a potential symmetry relation $\nabla_{r(T,t)}^s = \pm \nabla_T^s$, where t is a closed strand. For example, if



$\nabla_T^b = p^{-2}r - (r - r^{-1}) - p^2r^{-1}$. So in general, the theorem and its corollary above become false if we do not reverse the orientations of *all* strands in the tangle T_\circ when the orientations of the open strands needs to be reversed for a mutation.

Proof of theorem 3.3. We consider the same two cases as in corollary 3.2, and also use its notation. Denote by A, B, C and D the corresponding counterparts of a, b, c and d from $T \setminus T_\circ$, such that

$$\nabla_T^s = Aa + Bb + Cc + Dd.$$

If we rotate about the x -axis, we have to reverse orientations in both cases of corollary 3.2, so

$$\nabla_{T'}^s = Aa_{\text{rev}} + Bd_{\text{rev}} + Cc_{\text{rev}} + Db_{\text{rev}} = Aa + Bb + Cc + Dd = \nabla_T^s.$$

Next, let us consider rotations about the y -axis. In case i, we do not need to reverse orientations. We have

$$\nabla_{T'}^s = Ac + Bb + Ca + Dd = Aa + Bb + Cc + Dd = \nabla_T^s.$$

In case ii, we need to reverse orientations:

$$\nabla_{T'}^s = Ac_{\text{rev}} + Bb_{\text{rev}} + Ca_{\text{rev}} + Dd_{\text{rev}} = Aa + Bb + Cc + Dd = \nabla_T^s$$

Finally, note that rotation about the z -axis is the same as rotation about both the x - and the y -axis (in any order), so we are done. \square

4 Geometric interpretation of ∇_T^s

Recall that the classical Alexander polynomial of a knot or link L can be defined as follows: Let \tilde{X} denote the maximal Abelian cover of the link complement $X = S^3 \setminus L$. We have an action of $H_1(X)$ on \tilde{X} . Thus, we can regard $H_1(\tilde{X})$ as a module over the group ring of $H_1(X)$. Then, the Alexander polynomial is the determinant of any square presentation matrix of $H_1(\tilde{X})$.

We would like to give a similar geometric interpretation of our polynomial tangle invariants. But first, we do some basic calculations:

Lemma 4.1. *Let T be a tangle in B^3 with n open and m closed components. Then $H_1(B^3 \setminus T) \cong \mathbb{Z}^{n+m}$ is freely generated by the meridians of the tangle components and $H_2(B^3 \setminus T) \cong \mathbb{Z}^m$ is freely generated by the boundaries of tubular neighbourhoods of the closed tangle components.*

Proof. The Mayer-Vietoris sequence for the decomposition $B^3 = B^3 \setminus T \cup \nu(T)$, $\nu(T)$ being a tubular neighbourhood of T , gives isomorphisms

$$H_*(\coprod_n S^1) \amalg (\coprod_m T^2) \cong H_*(\partial\nu(T)) \rightarrow H_*(B^3 \setminus T) \oplus H_*(\nu(T)) \quad \text{for } * > 0.$$

Note that $\nu(T) \simeq (\coprod_n B^3) \amalg (\coprod_m S^1 \times D^2)$ and the longitude of any torus T^2 goes to the generator of the corresponding $H_1(S^1 \times D^2)$. \square

Next, we explicitly calculate the cellular chain complex of the tangle complement $X = B^3 \setminus T$ from a fixed tangle diagram T by considering the following handle decomposition: We start with two 0-handles, one sitting below and the other above the diagram. For each region, take a 1-handle from one 0-handle to the other. To simplify arguments below, we orient these 1-handles as follows: Choose a checkerboard colouring of the diagram and orient the 1-handles corresponding to one colour in one direction and the others in the opposite direction. Finally, for each crossing, attach a 2-handle to the 1-handlebody as illustrated in figure 5.

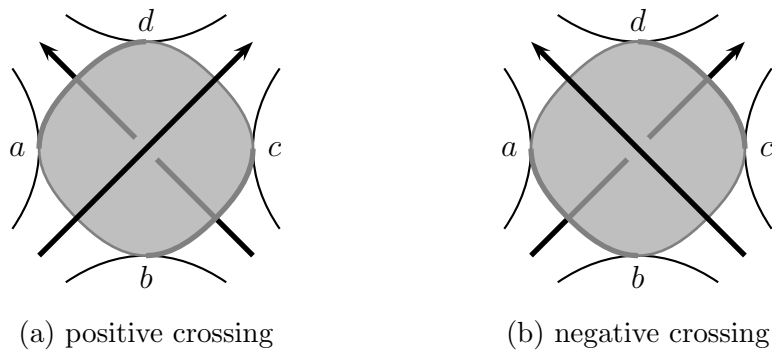


Figure 5: Attaching 2-handles at crossings

Here, a , b , c and d denote 1-handles. Up to an overall sign, the attaching map is then given by $a + b + c + d$ in both cases. This gives rise to the following cellular chain complex of X :

$$\mathbb{Z}^c \xrightarrow{A} \mathbb{Z}^{c+n+1} \longrightarrow \mathbb{Z}^2, \quad (2)$$

where c is the number of crossings, $c + n + 1$ the number of regions in the diagram and A is the $(c + n + 1) \times c$ matrix determined by the rules above. (Here, we assume that the diagram is connected and has at least one crossing.) Let $R = \mathbb{Z}H_1(X)$, the group ring of $H_1(X)$. Then the cellular chain complex of the maximal Abelian cover is

$$R^c \xrightarrow{\tilde{A}} R^{c+n+1} \longrightarrow R^2. \quad (3)$$

The attaching maps of the 1-handles, which determine the matrix \tilde{A} , are given by $a + o^{-1}b + o^{-1}c + d$ for positive crossings and $a + b + o^{-1}c + o^{-1}d$ for negative crossings up to multiplication by a unit in R , where o is the variable corresponding to the over-strand. Also note that we have used the right-hand rule to determine the exponents of these variables.

Each site s of a tangle diagram gives rise to a subhandlebody of X which we can regard as a subspace B_s of $(\partial B^3) \setminus T$: We associate with s the subhandlebody of X consisting of the two 0-handles and all 1-handles corresponding to those regions not in s , i. e. unoccupied open regions. The cellular chain complex of B_s is

$$\mathbb{Z}^{n+1} \longrightarrow \mathbb{Z}^2,$$

which we can consider as a subcomplex of (2). Similarly, we can consider the preimage \tilde{B}_s of B_s in \tilde{X} and regard its cellular chain complex as a subcomplex of (3). Then the quotients of these chain complexes calculate $H_*(X, B_s)$ and $H_*(\tilde{X}, \tilde{B}_s)$, respectively, and they are given by

$$\mathbb{Z}^c \xrightarrow{A_s} \mathbb{Z}^c \quad \text{and} \quad R^c \xrightarrow{\tilde{A}_s} R^c,$$

where A_s and \tilde{A}_s denote the matrices obtained from A and \tilde{A} by deleting those rows corresponding to s , respectively. Note that $H_1(\tilde{X}, \tilde{B}_s)$, considered as an R -module, is an invariant of $(\tilde{B}_s \subset \tilde{X})$, and \tilde{A}_s is just a presentation matrix of $H_1(\tilde{X}, \tilde{B}_s)$.

Proposition 4.2. *Let s be a site of a connected tangle diagram T . Let \tilde{A}_s be a presentation matrix of $H_1(\tilde{X}, \tilde{B}_s)$ as in the construction above. Then*

$$\det \tilde{A}_s(t_1^2, \dots, t_r^2) \doteq \nabla_T^s(t_1, \dots, t_r),$$

where \doteq denotes equality up to multiplication by a unit.

Observation 4.3. Let us verify this statement for knots and links. For a 2-ended tangle T representing a knot or link L , define $X := B^3 \setminus T \cong S^3 \setminus L$. Hence the first homology groups of the maximal Abelian covers are the same as $H_1(X)$ -modules. B_s is homotopic to the meridian of the open component, hence for knots, \tilde{B}_s is homotopic to the real line, so $H_1(\tilde{X}, \tilde{B}_s) = H_1(\tilde{X})$. The argument for links is slightly more complicated. This is to be expected because by remark 1.9, we should see an additional factor $(c - 1)$, where c is the variable corresponding to the single open strand.

Let us consider a slightly more general situation, where we have an arbitrary tangle T with a closed component c and we want to compare $H_1(\tilde{X}, \tilde{B}_s)$ with $H_1(\tilde{X}, \tilde{B}_s \amalg \tilde{M}_c)$, where M_c is a meridian of c . Given a diagram of T , consider the following handle-decomposition of X : Start with three 0-handles, one below the diagram on the boundary

of the closed 3-ball (e_-), one above (e_+) and one on M_c (e_c). Then add a 1-handle for each open region, connecting the two 0-handles above and below, a 1-handle m_c along M_c and a 1-handle j joining e_c to e_- , say. Finally, add a 2-handle along m_j , j and the two 1-handles corresponding to the two open regions on either side of M_c and additional 2-handles at the crossings as before. Let $R := H_1(X)$. For the maximal Abelian cover, we obtain the following chain complex:

$$R^a \xrightarrow{A} R^{a+n} \oplus Rm_c \oplus Rj \xrightarrow{B} Re_- \oplus Re_+ \oplus Re_c,$$

where matrix B takes the following form:

$$\begin{pmatrix} * & 0 & -1 \\ 0 & 0 & 0 \\ 0 & (c-1) & 1 \end{pmatrix}.$$

On the one hand, to get a presentation matrix $A_{B_s \amalg M_c}$ for $H_1(\tilde{X}, \tilde{B}_s \amalg \tilde{M}_c)$, we simply need to take the quotient of this complex with

$$R^{n+1} \oplus Rm_c \longrightarrow Re_- \oplus Re_+ \oplus Re_c,$$

where $R^{n+1} \subset R^{a+n}$ is generated by those 1-handles corresponding to the site s ; so we just need to delete certain rows in A . On the other hand, if we quotient only by a subcomplex of the previous one, namely

$$R^{n+1} \longrightarrow Re_- \oplus Re_+,$$

then the kernel of the right-hand map in the quotient complex

$$R^a \xrightarrow{A_q} R^{a+n}/R^{n+1} \oplus Rm_c \oplus Rj \xrightarrow{B} Re_c$$

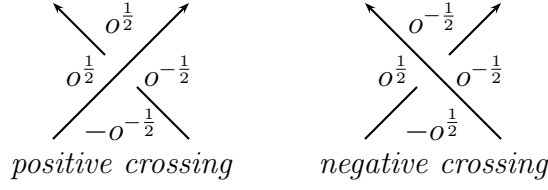
is $R^{a+n}/R^{n+1} \oplus R((c-1)j - m_c)$: Therefore, a presentation matrix A_{B_s} of $H_1(\tilde{X}, \tilde{B}_s)$ is obtained from A_q by deleting the row for m_c , multiplying the row for j by $(c-1)$ and subtracting the row for m_c from it. Note that the square matrix obtained from A_q by deleting the row for j is not invertible (m_c is not in the image of A_q) and hence its determinant vanishes. Now use linearity of the determinant with respect to rows to deduce that

$$\det(A_{B_s \amalg M_c}) = (c-1) \det(A_{B_s}).$$

We will use this argument later in the proof of theorem 6.22.

The proof of proposition 4.2 follows from basically the same argument as the corresponding statement for the classical Alexander polynomial, see [Kau83, Prop. 3.1]. The crucial point is that the signs in the definition of the determinant of a matrix and the signs coming from $h = -1$ in the Alexander codes correspond to one another. In order to see this, we make use of the generalised clock theorem again. We also need the following lemma to match the Alexander codes – and again, the generalised clock theorem is the key.

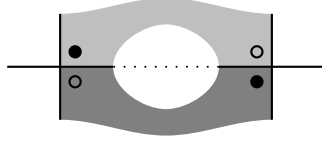
Lemma 4.4. *In definition 1.5, we can replace the Alexander codes from figure 4 by those below to obtain new polynomials $\nabla_{T,\text{new}}^s$.*



Then for all tangle diagrams T and sites s

$$\nabla_{T,\text{new}}^s(t_1^2, \dots, t_r^2) \doteq \nabla_T^s(t_1, \dots, t_r).$$

Proof. Using observation 1.6, we consider the effect of transposition moves on the labelling of the Kauffman states.



Let the variable corresponding to the horizontal strand be t . Note that any other variables are not affected by a transposition move. Now, if the two vertical strands go either both over or both under the horizontal strand, the two Kauffman states will have the same labelling for both codes. In the other case, the exponent of t will change by ± 1 for the code above, but by ± 2 for the original code. It is not hard to see that the signs are the same. Now apply the generalised clock theorem. \square

Definition 4.5. We define the **sign** $\text{sgn}(x)$ of a **Kauffman state** x of a connected tangle diagram to be the sign of $c(x)$ with $h = -1$, see definition 1.5.

Proof of proposition 4.2. Without loss of generality we may assume that at any crossing of the diagram, all four regions are pairwise distinct. For, once we have shown the above statement for this restricted case, it also holds true for any connected diagram, since both sides are invariants of T up to isotopy.

We can regard the Kauffman states as a region-crossing assignment, so we can fix a map $P : \mathbb{K}(T, s) \rightarrow S_n$. If x and y are two Kauffman states in $\mathbb{K}(T, s)$, $s \in \mathbb{S}(T)$, that are related by a transposition move, x and y have opposite signs. On the other hand, $P(x)$ and $P(y)$ also have opposite signs as elements of the permutation group. By the generalised clock theorem, we know that any two Kauffman states in $\mathbb{K}(T, s)$ are connected by a sequence of transposition moves. Hence $\text{sgn} = \pm \text{sgn} \circ P$. The proposition now follows from the definition of the determinant and lemma 4.4. \square

Corollary 4.6. *Let s be a site of a tangle T . Then*

$$\nabla_T^s(1, \dots, 1) = 0 \Leftrightarrow H_2(B^3 \setminus T, B_s) \neq 0.$$

Proof. Observe that the matrix A in (2) is obtained from the matrix \tilde{A} in (3) by setting all variables equal to 1. \square

Given two sites s and s' , B_s can be obtained from $B_{s'}$ by applying some element of the mapping class group of $\partial B^3 \setminus \partial T$. This means that if we know ∇_T^s for a fixed site s and all tangles T , we also know $\nabla_T^{s'}$ for all sites s' , up to normalisation. But why should we restrict ourselves to those subspaces B of the punctured sphere $\partial B^3 \setminus \partial T$ that come from sites? In principle, we can consider $H_1(\tilde{X}, \tilde{B})$ for any such B and define ∇_T^B to be the generator of the smallest principal ideal containing the first elementary ideal of $H_1(\tilde{X}, \tilde{B})$. This gives rise to infinitely many polynomial invariants ∇_T^B for any given tangle T . However, if for example $H_1(\tilde{X}, \tilde{B})$ has a presentation matrix with more columns than rows, i. e. more generators than relations, then ∇_T^B will be zero. This is for example always the case if $\chi(B) > (1 - n) = \chi(B^s)$.

These considerations give rise to the following proposition.

Proposition 4.7. *Let B be an essentially embedded subsurface of a $2n$ -punctured sphere, i. e. the map $\pi_1(B) \rightarrow \pi_1(\partial B^3 \setminus \partial T)$ induced by the inclusion is injective. Suppose further that $\chi(B) = 1 - n$. Then there exists an element g in the mapping class group of $\partial B^3 \setminus \partial T$ such that $g(B)$ is homotopic to B_s for some (and thus: any) site s .*

Proof. We fix some cellular structure on X with a single 0-cell such that B is a sub-cell-complex. We can arrange that the 1-cells are attached to the 0-cell in such a way that the ends of the every cell are neighboured. (They cannot be interleaved, so we can slide ends along the 1-cells.) Since B is essentially embedded, every 1-cell encloses at least one puncture. Hence, we can apply an element of the mapping class group of the punctured sphere such that the punctures enclosed by the same 1-cell are neighboured and similarly for those that are not enclosed by a 1-cell. Such a subspace can obviously be homotoped to some B^s . \square

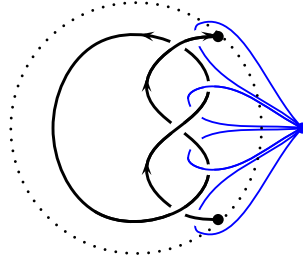
Questions 4.8. In the context of the proposition above, there are some open questions that we would like to answer; in particular:

- Can we describe higher elementary ideals of $H_1(\tilde{X}, \tilde{B}^s)$? What about ∇_T^B for the case $\chi(B) < 1 - n$?
- Can we compute the action of the mapping class group of $\partial B^3 \setminus \partial T$ on our invariants?
- What is the best way to normalise $\nabla_{T, new}^s$?
- Is there a geometric interpretation of the glueing formula from proposition 1.11, for example via some Mayer-Vietoris argument?

5 Comparison of ∇_T^s to other definitions

In the introduction, we mentioned several other generalisations of the Alexander polynomial to tangles. In this very short section, we try to compare our invariant to some of the other definitions. I hope to come back to this at some point in the future to make some of those vague statements below more precise.

Archibald’s invariant. In [Arc10], Archibald defines her polynomial Alexander invariant(s) for tangles directly via Alexander matrices. However, she uses a different cellular decomposition of the tangle complement to calculate the Alexander matrix; ours comes from the Dehn representation of the fundamental group of the complement, hers from the Wirtinger representation. For the latter, one fixes a single 0-cell above a tangle diagram and adds a loop for each connected arc in the diagram, as illustrated below.



These loops generate the fundamental group of the tangle complement. One then adds 2-cells, one for each crossing, which gives the relations between the generators. The columns of the Alexander matrix correspond to crossings as in our construction, but the rows correspond to arcs. Archibald then considers square matrices obtained by deleting some rows that correspond to arcs that meet the boundary, which we call “marked” arcs. A simple counting argument shows that we need to delete exactly n rows (if there are no closed arcs).

Let us assume for simplicity that every arc meets the boundary at most once. (We can always find such a diagram for a given tangle.) Then, those square matrices define a presentation of $H_1(\tilde{X}, \tilde{B})$, where B is the subspace of the boundary given by the 0-cell and those 1-cells corresponding to marked arcs. This subspace B does not necessarily have to be homotopic to one that comes from a site in our construction. However, after applying some element of the mapping class group of the boundary, it is, like in the last step of the proof of proposition 4.7. Thus, we can calculate Archibald’s invariant from our invariants and vice versa, up to normalisation.

Diagrammatic invariants. Using the skein relation for the one-variable Alexander polynomial and the convention that any diagram with an unknot component is zero, one can reduce any given tangle to a linear combination of “simpler” tangles. For a suitable (minimal) choice of such “elementary” tangles, this also gives an invariant. Since ∇_T^s also satisfies the skein relation, we can compute it by substituting the elementary tangles by their polynomials ∇_T^s . I assume that one can also go the other direction. For this, it would be sufficient to show that, given a minimal set of elementary tangles $\{T_i\}_i$, the matrix $(\nabla_{T_i}^s)_{i,s}$ has maximal rank. Since Bigelow’s [Big12] as well as Polyak’s [Pol10] invariants also satisfy the skein relation, this would imply that all of these polynomials contain basically the same information.

For the multivariate version, the same approach does not work. Computations suggest that ∇_T^s and Kennedy’s multivariate version [Ken12] of Bigelow’s invariant are closely related, but I have been unable to make this relationship precise. If we restrict ourselves to 4-ended tangles, in Proposition 3.1 we saw that there is basically only one piece of information in ∇_T^s . Kennedy’s invariant, consisting (a priori) of nine different polynomials, contains at most two different pieces of information, see [rel]. It would be interesting to know if one can make this result as strong as for ∇_T^s .

Sartori's invariant. I assume that one can interpret the tangle Floer homology defined in the next section as a special case of Ina and Vera's more general combinatorial tangle Floer homology [PV14], namely the one-sided case of tangles in D^3 ; this should follow more or less from the definition. Since their construction can be seen as a categorification of Sartori's invariant [EPV15], this would then imply a relationship between ∇_T^s and Sartori's one-sided invariant, taking the form of a map from a $U_q(\mathfrak{gl}(1|1))$ -representation V to $\mathbb{C}(q)$. Under this map, $\nabla_T^s(q)$ should be exactly the image of the element in V that corresponds to the site s in Ina and Vera's construction for tangles in D^3 .

6 Towards a categorification of ∇_T^s

6.1 A naive approach

Throughout this section, let T be a tangle with n open and no closed components and s a site of T . The complement of a tubular neighbourhood of the tangle in the closed 3-ball is denoted by X_T . In the following, we look at a definition of a tangle Floer theory that arises naturally from considering Heegaard diagrams for tangles. The following definition is motivated by example 6.2.

Definition 6.1. A **tangle Heegaard diagram** consists of the following data:

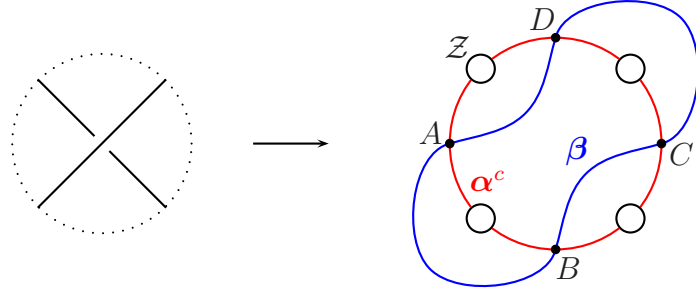
- An orientable surface Σ_g of genus $g \geq m$ with exactly $2n$ connected boundary components. We write $\partial\Sigma_g = \mathcal{Z}$;
- a set α^c of g pairwise disjoint curves $\alpha_1, \dots, \alpha_g$ on Σ_g ,
- a set α^a of $2n$ pairwise disjoint arcs $\alpha_1^a, \dots, \alpha_{2n}^a$ on Σ_g which are disjoint from α^c and whose endpoints lie on the circles in \mathcal{Z}^∂ , and
- a set β of $(g + n - 1)$ pairwise disjoint curves $\beta_1, \dots, \beta_{g+n-1}$ on Σ_g .

We write $\alpha := \alpha^c \cup \alpha^a$ and impose the following conditions on the data above:

- The surface $S_{\alpha^c}(\Sigma_g)$ obtained by surgery along the curves in α^c is a 2-sphere with $2n$ connected boundary components.
- The surface $S_\beta(\Sigma_g)$ obtained by surgery along the curves in β is a disjoint union of n annuli A_1, \dots, A_n .
- There are exactly two α -arc endpoints on each boundary circle in \mathcal{Z} and the α -arcs divide $S_{\alpha^c}(\Sigma_g)$ into two components, the “front” and the “back”.

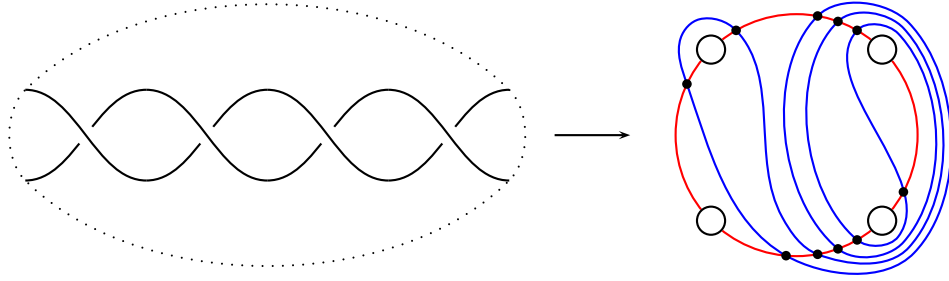
Remark. This data determines the tangle complement X_T as follows: Consider $\Sigma_g \times [0, 1]$ and attach a 2-handle along each $\alpha^c \times \{0\}$ and a 2-handle along each $\beta \times \{1\}$. The α -arcs correspond exactly to the circle on which the fixed ends of the tangle lie, see definition 1.1. Conversely, every tangle gives rise to a Heegaard diagram, which can be easily seen via Morse theory. However, this also follows immediately from the next example.

Example 6.2. For the one-crossing tangle, we draw the following Heegaard diagram:



For an arbitrary tangle diagram, we may draw the Heegaard diagram obtained by gluing Heegaard diagrams for one-crossings together along some components of \mathcal{Z} .

Example 6.3. For a rational tangle, we only need a single β -curve, as illustrated below:



In the following, let $\mathcal{H} = \mathcal{H}_T = (\Sigma_g, \mathcal{Z}, \alpha, \beta)$ be a Heegaard diagram for T .

Definition 6.4. Let $\mathbb{T} = \mathbb{T}_{\mathcal{H}}$ be the set of tuples $\mathbf{x} = (x_1, \dots, x_{g+n-1})$ of points $x_1, \dots, x_{g+n-1} \in \alpha \cap \beta$ such that there is exactly one point x_i on each α - and β -curve, and at most one point on each α -arc. \mathbb{T} will be the generating set of the chain module defined later on, so we call the tuples \mathbf{x} **generators**.

A **site** of a Heegaard diagram for a $2n$ -ended tangle is an $(n+1)$ -element subset of α^c . To each generator $\mathbf{x} \in \mathbb{T}$, we associate the site consisting of all those α -arcs that are occupied by an intersection point in \mathbf{x} . We denote the set of all generators corresponding to a given site s by \mathbb{T}^s . Thus, we obtain a partition of $\mathbb{T} = \coprod_{s \in \mathbb{S}} \mathbb{T}^s$ where $\mathbb{S} = \mathbb{S}(T)$ denotes the set of sites of the Heegaard diagram. This notation corresponds to that in definition 1.5.

We define the **group of domains** D to be the free group generated by the connected components of $\Sigma_g \setminus (\alpha \cup \beta \cup \mathcal{Z})$, which we call regions. In other words,

$$D = D_{\mathcal{H}} := H_2(\Sigma_g, \alpha \cup \beta \cup \mathcal{Z}).$$

Elements of this group are called **domains**.

Given two points $\mathbf{x}, \mathbf{y} \in \mathbb{T}$, we define $\pi_2(\mathbf{x}, \mathbf{y})$ to be the subgroup of those domains ϕ which satisfy

$$d(d\phi \cap \beta) = \mathbf{x} - \mathbf{y}.$$

We call elements in $\pi_2(\mathbf{x}, \mathbf{x})$ **periodic domains**. Note that this does not depend on the choice of $\mathbf{x} \in \mathbb{T}$. Furthermore, let

$$\pi_2^{\partial}(\mathbf{x}, \mathbf{y}) := \{\phi \in \pi_2(\mathbf{x}, \mathbf{y}) \mid \mathcal{Z} \cap \phi = \emptyset\}.$$

Lemma 6.5. *There is an isomorphism $\pi_2(\mathbf{x}, \mathbf{x}) \cong H_2(X_T, \mathcal{Z} \cup \alpha^a; \mathbb{Z}) \cong \mathbb{Z}^{n+1}$. Furthermore, $\pi_2^\partial(\mathbf{x}, \mathbf{x}) = 0$.*

Proof. By definition of periodic domains, we can write

$$\pi_2(\mathbf{x}, \mathbf{x}) = H_2(\Sigma_g \times [0, 1], \mathcal{Z} \times [0, 1] \cup \alpha \times \{0\} \cup \beta \times \{1\}; \mathbb{Z}).$$

We can now attach 2-handles to the α - and β -curves and use the fact that these 2-handles are contractible to see that the latter is isomorphic to $H_2(X_T, \mathcal{Z} \cup \alpha^a; \mathbb{Z})$, which is generated by the annuli which are boundaries of the tangle components and two discs, one at the front and the other at the back, the only relation being that the sum of the annuli is equal to the sum of the discs. \square

Lemma 6.6. *$\pi_2(\mathbf{x}, \mathbf{y})$ is nonempty for all pairs $(\mathbf{x}, \mathbf{y}) \in \mathbb{T}^2$.*

Proof. For any pair $(\mathbf{x}, \mathbf{y}) \in \mathbb{T}^2$, there exists a 1-cycle γ in $C_1(\alpha \cup \beta \cup \mathcal{Z})$ such that $d(\gamma \cap \beta) = \mathbf{x} - \mathbf{y}$. Indeed: First, choose a 1-chain on $C_1(\beta)$ with this property. Then, since there is exactly one intersection point on every α -curve for each \mathbf{x} and \mathbf{y} , we can add 1-chains in $C_1(\alpha^c)$ such that the boundary of the new 1-chain lies on the α -arcs only. But since γ is allowed to have \mathcal{Z} -components, we can get rid of these intersection points, too, and get our cycle γ .

Next, we can add \mathcal{Z} -cycles to γ such that the resulting 1-cycle is 0 in $H_1(Y)$. Adding α - and β -cycles gives us another 1-cycle γ' which is 0 in $H_1(\Sigma_g)$ and also satisfies $d(\gamma' \cap \beta) = \mathbf{y} - \mathbf{x}$. So we are done. \square

Next, we want to define an Alexander grading on generators. Our definition is very hands-on; we basically count \mathcal{Z} -components of domains connecting two generators which gives rise to a relative grading.

Definition 6.7. First, we define an Alexander grading on domains. In definition 6.10, we lift it to generators. Recall that, by definition, each circle in \mathcal{Z} has two components, a front and a back component. Let Σ_g^f , $(\alpha \cup \beta \cup \mathcal{Z})^f$ and α^f denote the spaces obtained from Σ_g , $(\alpha \cup \beta \cup \mathcal{Z})$ and α respectively by contracting the back component of each circle in \mathcal{Z} to a point. Note that $\beta \cap \mathcal{Z} = \emptyset$, $\alpha^c \cap \mathcal{Z} = \emptyset$ and that the images of α -arcs become a single circle in α^f . Let $f : (\alpha \cup \beta \cup \mathcal{Z}) \rightarrow (\alpha \cup \beta \cup \mathcal{Z})^f$ be the quotient map and $\partial : D \rightarrow H_1(\alpha \cup \beta \cup \mathcal{Z})$ the boundary map of the long exact sequence of the pair $(\Sigma_g, \alpha \cup \beta \cup \mathcal{Z})$. Now, consider the following diagram, where ι , ι^f , i and j are inclusions, and pr_2 is the projection onto the second summand:

$$\begin{array}{ccccc} D & \xrightarrow{\partial} & H_1(\alpha \cup \beta \cup \mathcal{Z}) & \xrightarrow{\iota} & H_1(\Sigma_g) & \xrightarrow{j} & H_1(Y) \cong H_1(\Sigma_g)/\langle \alpha^c, \beta \rangle \cong \mathbb{Z}^{n+m} \\ & & \downarrow f & \square & \downarrow \cong & \nearrow j^f & \uparrow \\ & & H_1((\alpha \cup \beta \cup \mathcal{Z})^f) & \xrightarrow{\iota^f} & H_1(\Sigma_g^f) & & \\ & & \cong \downarrow & & \uparrow i & \square & \\ & & H_1(\alpha^f \cup \beta) \oplus H_1(\mathcal{Z}^f) & \xrightarrow{\text{pr}_2} & H_1(\mathcal{Z}^f) & \xrightarrow{c = j^f \circ i} & \end{array}$$

Next, take some domain ϕ and consider $x := \partial\phi$ in $H_1(\alpha \cup \beta \cup \mathcal{Z})$. Then the image of $f(x)$ under the map ι^f is 0, and so is $j^f \circ \iota^f(f(x))$. However, we claim that if we just take

the \mathcal{Z}^f -components of $f(x)$, i.e. the image of $i(pr_2(f(x)))$ under j^f , we get something more interesting. We define a homomorphism

$$\mathbf{g}_{Alex}^f : D \rightarrow H_1(Y)$$

by $\mathbf{g}_{Alex}^f(\phi) := c(pr_2(f(\partial\phi)))$. Note that $H_1(Y)$ is generated by the images of \mathcal{Z} under $j \circ \iota$, so it is also generated by the images of \mathcal{Z}^f under c . For calculations, it is useful to think of an Alexander grading $\mathbf{g}_{Alex}^f(\phi)$ as an element in $H_1(\mathcal{Z}^f)/\ker(c)$.

We can do the same construction for contracting the front components to obtain a homomorphism

$$\mathbf{g}_{Alex}^b : D \rightarrow H_1(Y).$$

Lemma 6.8. \mathbf{g}_{Alex}^f and \mathbf{g}_{Alex}^b are constant on $\pi_2(\mathbf{x}, \mathbf{y})$ for all pairs $(\mathbf{x}, \mathbf{y}) \in \mathbb{T}^2$.

Proof. It suffices to show that periodic domains have Alexander grading $\mathbf{g}_{Alex}^f = 0$. But this is obvious from the description of the periodic domains in (the proof of) lemma 6.5. The annuli have cancelling \mathcal{Z} -boundary components of the corresponding tangle component and the \mathcal{Z} -boundary components of the two discs are the sums of all front/back \mathcal{Z} -components. \square

Lemma 6.9. $\pi_2^{\partial}(\mathbf{x}, \mathbf{y})$ is nonempty for all pairs $(\mathbf{x}, \mathbf{y}) \in \mathbb{T}^2$, if \mathbf{x} and \mathbf{y} are in the same Alexander grading and belong to the same site.

Proof. This follows from a careful refinement of the proof of 6.6: We can now get a 1-cycle γ in $C_1(\alpha \cup \beta)$ such that $d(\gamma \cap \beta) = \mathbf{x} - \mathbf{y}$, because the generators belong to the same site. This 1-cycle is already zero in $H_1(Y)$, since the generators are in the same Alexander grading. Then we might have to add α - and β -cycles as before and we are done. \square

Combining the lemmas 6.6 and 6.8 enables us to define a relative grading on \mathbb{T} .

Definition 6.10. The homomorphism $\mathbf{g}_{Alex} = \mathbf{g}_{Alex}^f + \mathbf{g}_{Alex}^b : D \rightarrow H_1(Y)$ induces a relative grading on \mathbb{T} , i.e. a map $\mathbf{g}_{Alex} : \mathbb{T} \rightarrow H_1(Y)$, uniquely defined by

$$\mathbf{g}_{Alex}(\phi) = \mathbf{g}_{Alex}(\mathbf{y}) - \mathbf{g}_{Alex}(\mathbf{x}), \text{ where } \phi \in \pi_1(\mathbf{x}, \mathbf{y}),$$

up to a constant. We write \mathbb{A} for the set of Alexander gradings and \mathbf{g}_{Alex}^r for the composition of \mathbf{g}_{Alex} with the map $H_1(Y) \rightarrow \mathbb{Z}$ that sends all meridians to 1. (“ r ” stands for “reduced”.)

For the homological grading, we use the usual formula, see for example [Srk06].

Definition 6.11. Let $\phi \in \pi_2(\mathbf{x}, \mathbf{y})$ for some $\mathbf{x}, \mathbf{y} \in \mathbb{T}$. Define

$$\begin{aligned} \mu(\phi) &= e(\phi) + m_{\mathbf{x}}(\phi) + m_{\mathbf{y}}(\phi), \text{ and} \\ \mathbf{g}_{hom}(\phi) &= \mu(\phi) - \frac{1}{2} \mathbf{g}_{Alex}^r(\phi), \end{aligned}$$

where $e(\phi)$ is the Euler measure of ϕ and $m_{\mathbf{x}}(\phi)$ and $m_{\mathbf{y}}(\phi)$ are the multiplicities of ϕ at \mathbf{x} and \mathbf{y} , respectively. More precisely, given a region ϕ of the Heegaard diagram, let $m_{\psi}(\phi)$ denote the multiplicity of ψ in ϕ . Then

$$m_{\mathbf{x}}(\phi) = \sum_{x_i \in \mathbf{x}} m_{x_i}(\phi),$$

where $m_x(\phi)$ is the average of the $m_{\psi_i}(\phi)$ in the four quadrants ψ_1, \dots, ψ_4 at x . Furthermore,

$$e(\phi) = \sum_{\text{regions } \psi} m_{\psi}(\phi) (\chi(\psi) - \frac{1}{4} \# \{\text{acute corners of } \psi\} + \frac{1}{4} \# \{\text{obtuse corners of } \psi\})$$

μ is called the Maslov index, \mathbf{g}_{hom} is the homological grading.

Lemma 6.12. *Given $\phi \in \pi_2(\mathbf{x}, \mathbf{y})$ and $\psi \in \pi_2(\mathbf{y}, \mathbf{z})$, $\mu(\phi) + \mu(\psi) = \mu(\phi + \psi)$*

Proof. This follows from basically the same arguments as [Srk06, Theorems 3.1 and 3.3]. We give some details nonetheless. First of all, note that the Euler measure is additive. Hence, all we need to show is that

$$m_{\mathbf{x}}(\phi) + m_{\mathbf{y}}(\phi) + m_{\mathbf{y}}(\psi) + m_{\mathbf{z}}(\psi) = m_{\mathbf{x}}(\phi + \psi) + m_{\mathbf{z}}(\phi + \psi).$$

This simplifies to

$$m_{\mathbf{y}}(\phi) + m_{\mathbf{y}}(\psi) = m_{\mathbf{x}}(\psi) + m_{\mathbf{z}}(\phi).$$

Theorem 3.1 from [Srk06] for $n = i = 2$, $\eta^1 = \alpha$ and $\eta^2 = \beta$ tells us that

$$m_{\mathbf{z}}(\phi) - m_{\mathbf{y}}(\phi) = \partial\phi \cdot \partial_{\beta}(\psi),$$

where the product \cdot denotes the “average” intersection number from [Srk06]. Similarly

$$m_{\mathbf{y}}(\psi) - m_{\mathbf{x}}(\psi) = \partial\psi \cdot \partial_{\beta}(\phi).$$

So we need to see that

$$\partial\psi \cdot \partial_{\beta}(\phi) = \partial\phi \cdot \partial_{\beta}(\psi)$$

or equivalently

$$\partial\psi \cdot \partial_{\beta}(\phi) + \partial_{\beta}(\psi) \cdot \partial\phi = 0.$$

The boundaries of the domains lie in $\alpha \cup \beta \cup \mathcal{Z}$. However, $\beta \cap \mathcal{Z} = \emptyset$, so the left-hand side equals $\partial_{\alpha}(\psi) \cdot \partial_{\beta}(\phi) + \partial_{\beta}(\psi) \cdot \partial_{\alpha}(\phi) = \partial_{\alpha \cup \beta}(\psi) \cdot \partial_{\alpha \cup \beta}(\phi)$. To see that this is zero, we modify the Heegaard surface by contracting all boundary components. Then the left-hand side is equal to $\partial(\psi) \cdot \partial(\phi)$, and this is indeed zero. \square

Lemma 6.13. *μ is constant on $\pi_2(\mathbf{x}, \mathbf{y})$ for all pairs $(\mathbf{x}, \mathbf{y}) \in \mathbb{T}^2$.*

Proof. Applying the previous lemma for $\mathbf{z} = \mathbf{y}$, we see that all we need to show is that

$$\mu(\phi) = e(\phi) + 2m_{\mathbf{y}}(\phi) \stackrel{!}{=} 0$$

for all periodic domains $\phi \in \pi_2(\mathbf{y}, \mathbf{y})$. We now use the explicit description of the elementary periodic domains from (the proof of) lemma 6.5. The correspondence between $\pi_2(\mathbf{x}, \mathbf{x})$ and $H_2(X_T, \mathcal{Z} \cup \alpha^a)$ is given by attaching/deleting 2-handles. So let us consider a periodic domain ϕ corresponding to an annulus. It consists of regions in Σ and discs from the 2-handles attached along α - and β -curves. For each α - and β -circle, there are 0, 1 or 2 such discs that belong to the annulus. Deleting such a disc from the annulus decreases the Euler measure by 1, but since each α - and β -circle is occupied by exactly one intersection point in \mathbf{x} , μ does not change. However, $\mu(\text{annulus}) = 0$, so the $\mu(\phi) = 0$, too. The same argument works for the two remaining elementary periodic domains, the discs. We only need to keep in mind that $(n-1)$ α -arcs are occupied, whose contribution is cancelled by the fact that there are $4n$ corners, so $e(\text{disc}) = 1 - n$. \square

Definition 6.14. Just as for the Alexander grading, we can now define a relative homological grading on generators. Combining lemmas 6.12 and 6.13, we define a \mathbb{Z} -grading by

$$\mathbf{g}_{\text{hom}}(\mathbf{y}) - \mathbf{g}_{\text{hom}}(\mathbf{x}) = \mathbf{g}_{\text{hom}}(\phi), \quad \text{where } \phi \in \pi_2(\mathbf{x}, \mathbf{y}).$$

Remark. By additivity of both the Alexander and the homological grading, the gradings are compatible with glueing.

Definition 6.15. We define the chain module $\widehat{CFT}(\mathcal{H})$ to be the \mathbb{Z} -module freely generated by the elements in \mathbb{T} . $\widehat{CFT}(\mathcal{H})$ carries two gradings, the Alexander grading and the homological grading, induced by the gradings on generators. We write $\widehat{CFT}(\mathcal{H}, s)$ for the submodule generated by those elements in \mathbb{T}^s and $\widehat{CFT}(T, s, a)$ for the submodule generated by those elements in \mathbb{T}^s of Alexander grading $a \in \mathbb{A}$. We define a differential on $\widehat{CFT}(\mathcal{H})$ by

$$\partial \mathbf{x} = \sum_{\mathbf{y} \in \mathbb{T}} \sum_{\substack{\phi \in \pi_2^\partial(\mathbf{x}, \mathbf{y}) \\ \mu(\phi)=1}} \# \mathcal{M}(\phi) \cdot \mathbf{y},$$

where $\# \mathcal{M}(\phi)$ denotes the usual signed count of certain holomorphic discs associated to ϕ ; for details, see for example [Juh06]. Note that there are no domains that avoid $\partial \Sigma$ between generators in distinct Alexander gradings or sites, so the chain module $\widehat{CFT}(\mathcal{H})$ admits a splitting into summands $\widehat{CFT}(\mathcal{H}, s, a)$.

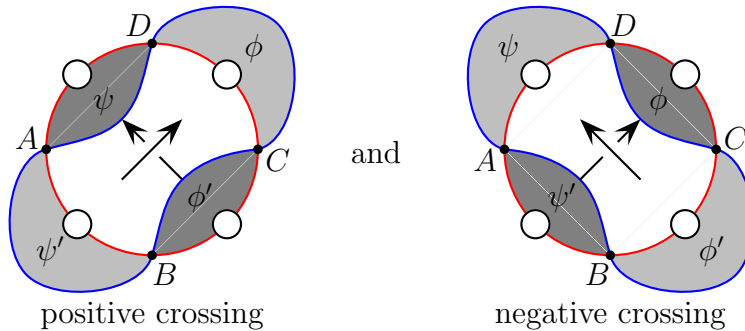
Theorem 6.16. ∂ in the definition above is indeed a differential. Furthermore, the chain homotopy type of $(\widehat{CFT}(\mathcal{H}_T, s, a), \partial)$ is an invariant of the tangle T .

Definition 6.17. Given a tangle T with no closed components, we define $\widehat{HFT}(T)$ to be the homology of the chain complex $(\widehat{CFT}(\mathcal{H}_T), \partial)$, where \mathcal{H}_T is some Heegaard diagram of T . We also write

$$\widehat{HFT}(T) = \bigoplus_{s \in \mathbb{S}(T)} \widehat{HFT}(T, s) = \bigoplus_{\substack{s \in \mathbb{S}(T) \\ a \in \mathbb{A}}} \widehat{HFT}(T, s, a).$$

Corollary 6.18. The graded Euler characteristic of the chain module $\widehat{CFT}(\mathcal{H}_T, s)$ coincides with the polynomial invariant ∇_T^s up to normalisation.

Proof. We first calculate the gradings of the generators for the one-crossing diagrams.



The Alexander grading \mathbf{g}_{Alex} of the regions ϕ , ψ , ϕ' and ψ' induce the same Alexander grading on generators used in the Alexander codes in figure 4. The Euler measures of the domains are all 0. Then, using the right-hand rule to determine the orientations of the \mathcal{Z} -circles, we see that in both cases

$$\mathbf{g}_{hom}(\phi) = \mathbf{g}_{hom}(\psi) = 0 \quad \text{and} \quad \mathbf{g}_{hom}(\phi') = \mathbf{g}_{hom}(\psi') = 1.$$

Finally, for a general tangle, we consider its “standard” Heegaard diagram discussed in example 6.2. Then, additivity of the Alexander and the homological grading shows that the Alexander grading of a generator in the whole diagram is the sum of the gradings in the local diagrams at the crossings. \square

Remark. The Mathematica program [nb] explicitly computes the generators of the categorified tangle invariant from a standard Heegaard diagram as in the proof above.

Definition 6.19. Corollary 6.18 allows us to promote the relative Alexander grading on \mathbb{T}^s to an absolute grading: We simply ask for the Euler characteristic of $\widehat{CFT}(\mathcal{H}_T, s)$ to agree with ∇_T^s . This fixes the Alexander grading as long as $\nabla_T^s \neq 0$.

Our proofs that ∂ is indeed a differential and that $\widehat{HFT}(T, s)$ is an invariant are both based on the following observation which identifies our tangle Floer homology with the sutured Floer homology of some suitable 3-manifold with boundary. For details on sutured Floer theory, see for example Juhász’ original paper [Juh06].

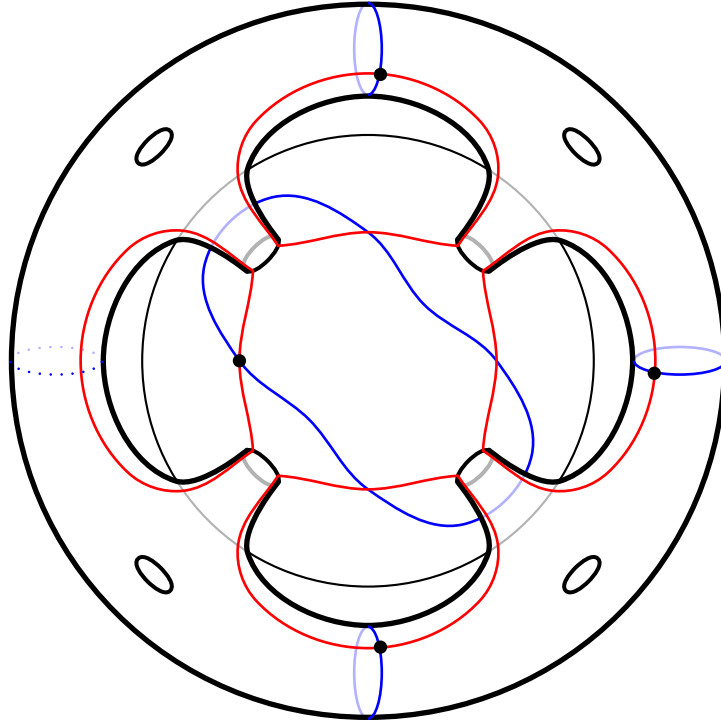


Figure 6: From a tangle Heegaard diagram to a sutured Heegaard diagram. This illustrates observation 6.20. In this example we see the Heegaard diagram for the one-crossing tangle. The dotted blue circle denotes the β -circle that is not in the diagram corresponding to the site of the shown generator.

Observation 6.20. Consider a 2-torus with a longitude and $2n$ disjoint meridians. Puncture the torus $2n$ times along the longitude such that any two meridians are no longer homotopic. We consider the arcs from the longitude as α -arcs and the meridians as β -curves. Note that each β -curve intersects exactly one α -arc in exactly one point and there are exactly $2n$ connected components in their complement on the punctured torus. Place a puncture in each of these components. Finally, we attach the (now $4n$ -punctured) torus to Σ in such a way that each α -arc in the torus closes an α -arc in Σ . We thereby obtain a sutured Heegaard diagram $\overline{\mathcal{H}}$ consisting of a $2n$ -punctured surface $\overline{\Sigma}$ with $(g+2n)$ α -circles and $(g+2n+n-1)$ β -circles. Figure 6 illustrates this construction. Next, fix a site s . s corresponds to the set of α -arcs in \mathcal{H} that are occupied by a generator in \mathbb{T}^s . An α -arc in \mathcal{H} corresponds to an α -arc in the punctured torus which in turn corresponds to the β -curve that it intersects. Let $\overline{\mathcal{H}}^s$ be the Heegaard diagram obtained by deleting those β -curves corresponding to α -arcs in s . Now observe that generators in \mathbb{T}^s correspond to generators in $\overline{\mathcal{H}}^s$ in the usual Heegaard Floer theory sense and that domains in \mathcal{H} that avoid \mathcal{Z} correspond to domains in $\overline{\mathcal{H}}^s$ that avoid $\partial\overline{\Sigma}$. Also, since the Alexander grading of those domains is 0, the Maslov indices agree. Hence $\widehat{HFT}(T, s)$ is identical to the sutured Floer homology $SFH(\overline{\mathcal{H}}^s)$.

$\overline{\mathcal{H}}^s$ represents the complement of a tubular neighbourhood of the union of the tangle T and those α -arcs that are in s pushed inside the closed 3-ball. The sutures are given by $\partial\overline{\Sigma}$. The diffeomorphism type of this sutured 3-manifold is obviously a tangle invariant.

Proof of theorem 6.16. By the observation above, all we need to check is that $\overline{\mathcal{H}}^s$ is admissible. But this is clear from the second statement of lemma 6.5. \square

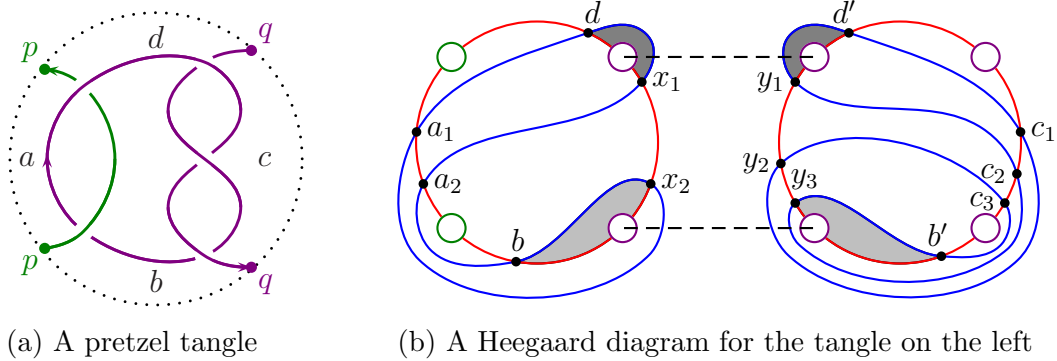


Figure 7: Illustration for example 6.21

Example 6.21. We compute our tangle Floer homology for the pretzel tangle of figure 7. The shaded regions show the only two domains that contribute to the differential that lead to the cancellation in the table of the generators and their gradings below:

site a	site b	site c	site d
$a_1y_1 : p^0 q^{+3} \delta^{\frac{1}{2}}$	$by_1 : p^{-1} q^{+1} \delta^0$	$x_1c_1 : p^{+1} q^{+2} \delta^{\frac{1}{2}}$	$dy_1 : p^{+1} q^{+3} \delta^0$
$a_1y_2 : p^0 q^{+1} \delta^{\frac{1}{2}}$	$by_2 : p^{-1} q^{-1} \delta^0$	$x_1c_2 : p^{+1} q^0 \delta^{\frac{1}{2}}$	$dy_2 : p^{+1} q^{+1} \delta^0$
$a_1y_3 : p^0 q^{-1} \delta^{\frac{1}{2}}$	$by_3 : p^{-1} q^{-3} \delta^0$	$x_1c_3 : p^{+1} q^{-2} \delta^{\frac{1}{2}}$	$dy_3 : p^{+1} q^{-1} \delta^0$
$a_2y_1 : p^0 q^{+1} \delta^{\frac{1}{2}}$	$x_1b' : p^{+1} q^{-3} \delta^1$	$x_2c_1 : p^{-1} q^{+2} \delta^{\frac{1}{2}}$	$x_1d' : p^{+1} q^{+3} \delta^1$
$a_2y_2 : p^0 q^{-1} \delta^{\frac{1}{2}}$	$x_2b' : p^{-1} q^{-3} \delta^1$	$x_2c_2 : p^{-1} q^0 \delta^{\frac{1}{2}}$	$x_2d' : p^{-1} q^{+3} \delta^1$
$a_2y_3 : p^0 q^{-3} \delta^{\frac{1}{2}}$		$x_2c_3 : p^{-1} q^{-2} \delta^{\frac{1}{2}}$	

It is now interesting to note that if we set $t := p = q$, then the result for the sites a and c are the same and for the sites b and d are the same after reversing the orientation $t \leftrightarrow t^{-1}$. For invariance under mutation by rotating the tangle by π in the plane, we need however $b = d$, which is only true for the δ -graded invariant.

Remark. Can we generalise the constructions above to tangles with closed components? In [Zib15], I showed that the above construction carries through for closed components as well, by enlarging the set of meridional circles \mathcal{Z} , except that I only got a $\mathbb{Z}/2$ homological grading and that I was unable to show that the chain homotopy type is an invariant of the tangle. I assume that the former could be fixed, but the latter cannot.

A “cheap” solution for closed components would be to increase the number of basepoints, i.e. add two punctures and an extra pair of α - and β -curves in such a way that each closed component gets two sutures. However, this multiplies the number of generators by 2^m and the Euler characteristic by a factor $(c - c^{-1})$ for each closed component c . This is essentially done in the next subsection.

6.2 A categorification via sutured Heegaard Floer theory

In the following, we offer a shortcut to the construction in the preceding subsection, which extends our tangle Floer homology to tangles with closed components.

Theorem 6.22. *Let T be a tangle and s a site of T . Let X_T^s be the sutured 3-manifold, whose underlying 3-manifold with boundary is the tangle complement and whose sutures are obtained by placing two oppositely oriented meridional circles around closed components of the tangle and meridional circles around the ends of the open components and performing surgery along those arcs in s . We orient the sutures such that one component of R_- is contained in the boundary of the 3-ball. Then the sutured Floer homology $SFH(X_T^s)$ is an invariant of the tangle T and the site s . Furthermore,*

$$\chi(SFH(X_T^s))(t_1^2, \dots, t_r^2) \doteq \prod (c - c^{-1}) \cdot \nabla_T^s(t_1, \dots, t_r), \quad (4)$$

where the product on the right is over all closed components c of T . Finally, for tangles without closed components, the $SFH(X_T^s)$ agrees with $\widehat{HFT}(T, s)$.

Observation 6.23. The final part can be seen very easily by comparing the sutured manifolds defined here to those from observation 6.20. We can obtain the former from the latter by cutting out product 1-handles at those open regions of the diagram that belong to the site. Since adding/cutting product 1-handles does not change sutured Floer homology, the construction here agrees with the one in the previous subsection, for tangles without closed components. However, we give a completely independent proof of the theorem, making use of our geometric interpretation of ∇_T^s from section 4.

Specialising to 2-ended tangles T that represent a knot or a link L , we observe that X_T^\emptyset is simply the knot/link complement with two meridional sutures on each component, so $SFH(X_T^\emptyset)$ agrees with ordinary link Floer homology $\widehat{HFL}(T)$ by [Juh06, Proposition 9.2].

Remark 6.24. The sutured Floer homology of any sutured manifold (M, γ) comes with two gradings: an absolute grading by relative Spin^c -structures of (M, γ) and for each such Spin^c -structure, a relative homological $\mathbb{Z}/2$ -grading. If we restrict to tangles without closed components then $H_2(X_T^s) = 0$, so we can lift the relative homological grading to

a relative \mathbb{Z} -grading using [Juh06, theorem 5.5]. However, by using the same idea as in the proof of lemma 6.13, we can also do this in the case of closed components and define an *overall* relative homological \mathbb{Z} -grading.

Note that the Alexander grading for the previous construction was a relative $(\frac{1}{2}\mathbb{Z})^{|T|}$ -grading *for all sites s simultaneously*. To achieve this purely in terms of sutured Floer homology, one would have to relate relative Spin^c -gradings corresponding to different sites, i. e. sets of sutures.

Proof of theorem 6.22. We first check that X_T^s is balanced. Say T has n open components and without loss of generality, we may assume that there are no closed components. The site s consists of $(n - 1)$ open regions, so there are $(n - 1)$ arcs that we have performed surgery along. Hence, R_- is a sphere with $(n + 1)$ punctures, so it has Euler characteristic $(1 - n)$. Each annulus around an open tangle component contributes 0 to the Euler characteristic, but each surgery decreases the Euler characteristic by 1.

Obviously, X_T^s is an invariant of T , and so is its sutured Floer homology. So it only remains to check the identity (4). For this, we use the explicit formula for $\chi(SFH(M, \gamma))$ of a sutured manifold (M, γ) via Fox calculus from [FJR09, Proposition 5.1]: Consider the pair (M, R_-) and its maximal Abelian cover (\tilde{M}, \tilde{R}_-) . Let A be a square presentation matrix of $H_1(\tilde{M}, \tilde{R}_-)$ as a $H_1(M, R_-)$ -module. Then $\chi(SFH(M, \gamma))$ is equal to $\det(A)$. We have basically done all the work in the previous section. First, suppose T does not have a closed component. Then, using the notation from proposition 4.2, $H_1(X_T^s, R_-) \cong H_1(B^3 \setminus T, B_s)$ and the same holds for the maximal Abelian covers, so we are done by the same proposition. For the general case, we get a factor $(c - c^{-1})$ for each closed component by observation 4.3. \square

The following results should be compared to their counterparts in sections 2 and 3.

Proposition 6.25. *Let $m(T)$ denote the mirror image of a tangle T . Then*

$$\widehat{CFT}(m(T), s, a) \cong \widehat{CFT}^*(T, s, -a).$$

Proof. This follows from the previous theorem and [FJR09, proposition 2.14]. \square

Proposition 6.26. *Let T be an oriented r -component tangle. If $r(T, t_1)$ denotes the same tangle T with the orientation of the first strand reversed, then for all sites $s \in \mathbb{S}(T)$, homological grading h and Alexander grading $a = (a_1, \dots, a_r)$,*

$$\widehat{CFT}_h(r(T, t_1), s, a) \cong \widehat{CFT}_{h-a_1}(T, s, (-a_1, a_2, \dots, a_r)).$$

Proof. This is immediate from the definition of the gradings from subsection 6.1. \square

Corollary 6.27. *Let T be an oriented r -component tangle. If $r(T)$ denotes the same tangle T with the orientation of all strands reversed, then for all sites $s \in \mathbb{S}(T)$, homological grading h and Alexander grading a ,*

$$\widehat{CFT}_h(r(T), s, a) \cong \widehat{CFT}_{h-a}(T, s, -a).$$

Proposition 6.28. *Let T be a 4-ended tangle. We distinguish between the same two cases as in proposition 3.1:*



Then in both cases,

$$\widehat{HFT}(T, b) = \widehat{HFT}(r(T), d). \quad (\text{B-D})$$

In case II, we also have

$$\widehat{HFT}(T, a) = \widehat{HFT}(r(T), c). \quad (\text{II A-C})$$

Proof of proposition 6.28. Using the observation above, the relations (B-D) and (II A-C) follow quite easily, because in both cases, we can push the two meridional sutures through the tangle to see that both sutured manifolds are the same, except for the fact that we have reversed the orientations of the sutures, i.e. we have switched the roles of R_- and R_+ . By [FJR09, Proposition 2.14], the sutured Floer homologies are identical, except that the Spin^c -grading is reversed. This together with proposition 6.26 finishes this proof. \square

Remark 6.29. Proposition 3.1 suggests that we might also expect other relations, in particular the relation

$$V_p \otimes \widehat{HFT}(T, a) = V_q \otimes \widehat{HFT}(T, c) \quad (\text{I A-C})$$

in case I, where V_t denotes a 2-dimensional vector space supported in grading t and $h^{\pm 1}t^{-1}$.

Appendix: The proof of the generalised clock theorem

First of all, we introduce some terminology, some of which is inspired by [Kau83]:

Definition A.1. A **D-graph** is a planar graph embedded in the closed disc D^2 such that at least one vertex lies on ∂D^2 .

Definition A.2. A **universe** is a D-graph such that all vertices in the interior of D^2 are 4-valent and the ones on ∂D^2 are 1-valent. A **face** of a graph embedded into D^2 is a connected component of the complement of this graph in D^2 .

Remark. We define generalised Kauffman states of universes just as for tangles. In fact, a universe is obtained from a tangle diagram by forgetting the under/over information at each crossing, and conversely, any universe gives rise to some tangle diagram.

Definition A.3. For a given tangle/universe, a **clocked state** is a generalised Kauffman state with the property that one cannot perform any counter-clockwise transposition move.

The generalised clock theorem (theorem 1.13) follows immediately from the following two propositions and their duals.

Proposition A.4. *In any universe one cannot perform an infinite number of clockwise transposition moves in sequence.*

Proposition A.5. *The set of Kauffman states of a fixed site of a universe has a unique clocked state if it is not empty.*

Proof of the generalised clock theorem. If the set of Kauffman states for a given site is empty, there is nothing to show. Otherwise, given any two Kauffman states x and x' of a fixed site, proposition A.4 gives us two clocked states y and y' with $x \leq y$ and $x' \leq y'$. Proposition A.5 tells us that $y = y'$, so the set of Kauffman states of a fixed site is a (finite) join-semilattice.

The duals of propositions A.4 and A.5 follow from considering mirror diagrams and observing that the mirror of a clockwise transposition move is a counter-clockwise transposition move and vice versa. Thus we see that the set of Kauffman states of a fixed site is also a (finite) meet-semilattice and the result follows. \square

Proof of proposition A.4. The argument from [GL86, Lemma 4] carries over to the tangle case; for completeness, we recall it here: First of all, note that transposition moves do not change sites. Hence, the marker of an outermost vertex, i.e. one which meets an open unoccupied region, cannot make a complete cycle. A marker at a vertex which has a common edge with an outermost vertex cannot make two cycles because in the course of each cycle it has to interact with the marker at the outermost vertex and that one cannot make a full cycle. Similarly, a marker at a vertex which is $n = 2$ edges away from an outermost vertex cannot make $2^n = 2^2 = 4$ full cycles, and so on. \square

For proposition A.5, we first generalise the correspondence used in [GL86] between spanning trees and states, see also [Kau83, Theorem 2.4].

Given a connected oriented universe U , partition the set of faces of U into two subsets by shading each component which is separated from an arbitrarily fixed region by an odd

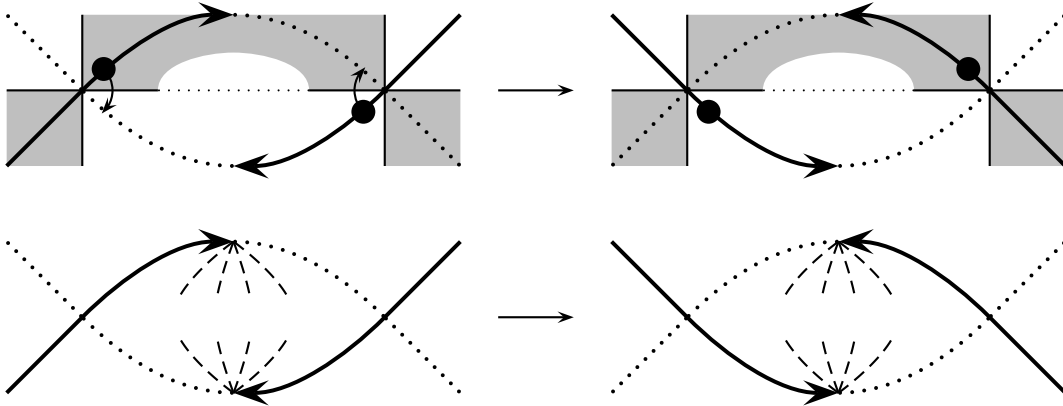
number of edges. Form a new D-graph $G(U) = G$ with one vertex for each shaded region and one edge for each crossing shared by these shaded regions, such that the vertices lie in their corresponding regions and those vertices of all open regions lie on ∂D^2 . In a similar way, we obtain a D-graph H from the unshaded regions. Note that H is the dual graph of G .

Definition A.6. Given a D-graph G and its dual G^* , a **D-forest** F is the union of a maximal forest F_G in G and its dual F_G^* in G^* such that each forest has at least one point on ∂D^2 , together with a specification of a root on ∂D^2 for each tree in F .

Lemma A.7. *There is a one-to-one correspondence between D-forests in $G(U)$ and Kauffman states of a (connected) universe U .*

Proof. The argument from [Kau83, Lemma 2.4] carries over, but we spell this out explicitly nonetheless. Given a D-forest F , we orient its edges in the canonical way, that is arrows point away from the roots. For each edge of F , place a marker into the region that the arrow of the edge is pointing towards. We claim that this defines a valid Kauffman state. Indeed, for each vertex in F except the roots there is exactly one arrow pointing towards this vertex. Since vertices in F correspond one-to-one to faces of U , we are done. Going from Kauffman states back to forests in G is now straightforward: For each marker at a crossing, we draw an edge between the corresponding vertices, according to the rule used above. Note that at each crossing, there is exactly one edge, so we get two disjoint subgraphs, one in $G(U)$ and one in $G(U)^*$. There is no simple cycle in either of these subgraphs. Otherwise, there would be a subdiagram D' traced out by the cycle in D^2 . A simple Euler characteristic argument leads to a contradiction: Say, there are n vertices in this cycle (each of which becomes a 2-valent vertex in D') and m crossings of U in D' . Then we have a total of $(m + n)$ vertices, $2(m + n)$ edges and therefore $1 + 2(m + n) - (m + n) = (m + n + 1)$ faces in D' . Only the inner faces need to be occupied by markers, which means m markers have to occupy $(m + 1)$ faces. Contradiction. Finally, every unoccupied region of U becomes a root in F . It is clear that every tree in F has exactly one root. \square

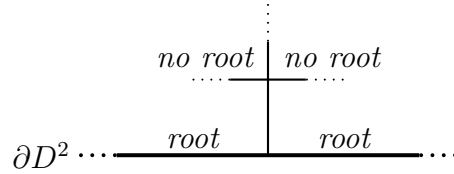
Next, we need to describe what a transposition move looks like in the language of D-forests. The following picture illustrates the clockwise transposition move. The dotted edges denote those edges in the graph G and its dual G^* that do not belong to the forest. The dashed edges denote edges in the graph that may or may not be in the forest.



We are now ready to give an outline of the proof of proposition A.5. The proof goes by induction on the number of crossings in a tangle diagram. The induction step relies on the fact that a certain edge of the graph G belongs to any clocked forest. This is the content of the next proposition.

Proposition A.8. *For any site of a (connected) universe, there exists a pair of two adjacent roots with the following property: For all $r \geq 0$, the number of roots in the next $2r$ boundary faces (moving counter-clockwise along the boundary, that is to the right of the picture below, see also figure 8) contain at least r roots.*

Furthermore, suppose we have a site of a connected universe together with two such roots. Since the diagram is connected, we can consider the first crossing that one reaches along their common edge from the boundary of the disc. Suppose the two other regions at this crossing are no roots, as in the following picture.



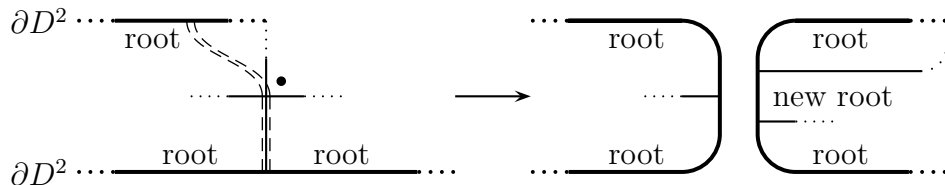
Then the marker of the crossing in the picture above sits in the upper left region for any clocked Kauffman state of this universe with respect to the fixed site.

We postpone the proof of proposition A.8 and first see how it implies proposition A.5.

Proof of proposition A.5. The start of the induction is given by all those tangle diagrams that have exactly one Kauffman state. For these, the statement is trivially true.

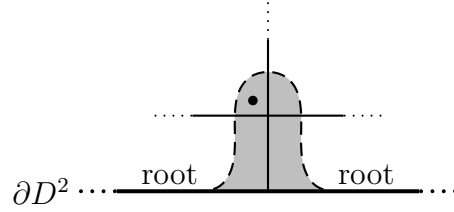
For the induction step, consider a universe U and a clocked Kauffman state x of U . Without loss of generality, we may assume that the diagram is connected. Indeed: Otherwise we can consider its connected components by splitting the diagram at a region with more than one component on ∂D^2 and repeating this process as often as necessary. Observe that the restrictions x_i of x to the connected diagrams are also clocked and that the sites of the restrictions of any other (clocked) Kauffman state of the same site as x agree with the sites of the x_i . Hence, if we can show the proposition for the x_i , then it also holds for x .

Now, consider two adjacent roots and the first crossing that one reaches along their common edge from the boundary of the disc. Obviously, not all four regions of this crossing can be roots. If there is exactly one additional root at this crossing, one can split the diagram into two parts like so:



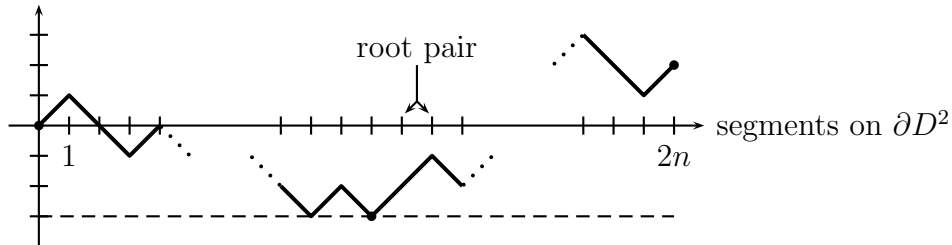
Note that the marker at the crossing has to be where it is for any Kauffman state. Also note that this splitting reduces the number of crossings by 1, so we can apply the induction hypothesis to both diagrams and we are done. So without loss of generality, we may now also assume that all adjacent roots locally look as in proposition A.8.

We consider the subdiagram obtained by removing a small neighbourhood of the edge from the boundary to this crossing. The clocked Kauffman state x restricts to a clocked Kauffman state $x|$ of the subdiagram.

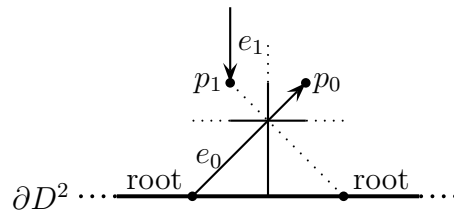


The subdiagram has one crossing fewer and we can apply the induction hypothesis, i. e. $x|$ is the unique clocked Kauffman state of the subdiagram with respect to the site of x . Since this site is uniquely determined by the site of x and the marker in the picture above, x is the unique clocked Kauffman state of the universe U with respect to the site of x . \square

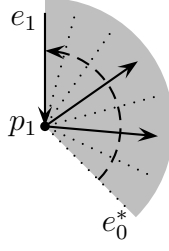
Proof of proposition A.8. The existence of a pair of roots with the special property required above follows from a standard argument: Consider the $2n$ line segments on ∂D^2 , choose one as a starting point and walk along ∂D^2 in counter-clockwise direction. Define a function from the set of segments to \mathbb{Z} by adding $+1$ for each root segment and -1 for an occupied segment, see the illustration below. The value of the function at the very last segment will be 2. Then consider the rightmost segment where the function takes its minimum. This will be a non-root, followed by two successive roots. By construction, these have the required property.



Let us denote the vertex corresponding to the upper right (resp. left) region of the picture in proposition A.8 by p_0 (resp. p_1). Suppose the edge from the right root to p_1 does not belong to the D -forest F corresponding to a clocked Kauffman state. We want to show that somewhere in the diagram, we can perform a counter-clockwise transposition move, so x cannot be a clocked state. Let us call its dual (which is in the D -forest) e_0 . Then e_0 points away from the left root:



Note that p_1 has (exactly) one incoming edge e_1 of F , since p_1 is not a root. Consider the edges in F that the dual e_0^* of e_0 meets on its way to e_1 during a counter-clockwise rotation around p_1 , see the picture below. (Note that there might be no such edge.)



Let F' be the tree consisting of p_1 , these edges and all vertices and edges in F that can be reached from these edges when following the arrows. Then the special property of our chosen pair of adjacent edges enables us to prove the following:

Lemma A.9. *Any vertex q that belongs to F' does not lie on ∂D^2 .*

Proof. Suppose there is such a vertex q . Note that $p_1 = q$ is also allowed. We have the following situation:

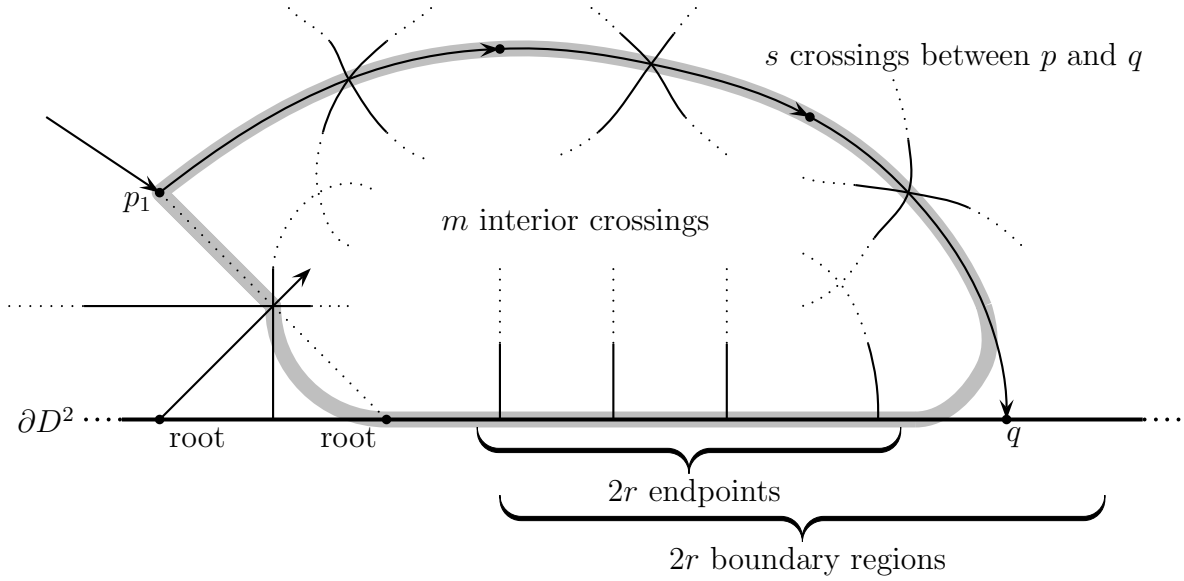


Figure 8: Euler characteristic argument for lemma A.9.

We compute the number of faces of the disc enclosed by the grey curve, using an Euler characteristic argument. There are m interior crossings, say, $2r$ endpoints on the boundary between q and the right root, and s crossings between p_1 and q . (Again, $s = 0$ is allowed.) Then we have

$$\begin{aligned}
\#\{\text{vertices}\} &= 2r + s + 2 + m \\
\#\{\text{edges}\} &= (2r - 1) + s + 3 + \frac{1}{2}(4m + 2r + 2s + 2) \\
&= 3r + 2s + 3 + 2m \\
\Rightarrow \#\{\text{faces}\} &= 1 + \#\{\text{edges}\} - \#\{\text{vertices}\} = r + s + 2 + m
\end{aligned}$$

Hence the number of occupied faces is

$$\#\{\text{faces}\} - (s + 1) - (\geq r + 1) \leq m.$$

However,

$$\#\{\text{markers}\} = m + 1.$$

Contradiction! □

Corollary A.10. *The vertex p_2 that we reach by following the dual edge of e_1 to the left of e_1 is in the full subtree starting at p_0 (see figure 9).*

Proof. Choose a small contractible neighbourhood of the tree F' . Then its boundary gives us a path in D^2 from the region corresponding to the vertex p_0 to the region containing p_2 that is disjoint from the D -forest F . □

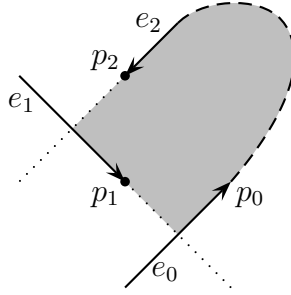
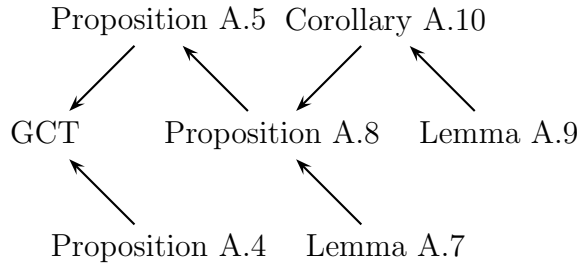


Figure 9: The iteration step

We can now finish our proof of proposition A.8. The corollary above tells us in particular that p_2 is not a root, so there is exactly one incoming edge e_2 . Note that if $p_0 = p_2$ (or equivalently $e_0 = e_2$), we are done, because we can perform a counter-clockwise transposition move. If $p_0 \neq p_2$, we can repeat the argument for p_2 in place of p_1 . It is now clear that p_3 is in the subtree starting at p_1 and therefore has an incoming edge. This is where we needed the lemma in the first iteration step.

This algorithm terminates because there are only finitely many vertices in the shaded region in figure 9 and the number of vertices in the corresponding shaded area in each iteration step strictly decreases unless the algorithm terminates during this step. □

This finishes the proof of the generalised clock theorem. The line of argument is summarised below:



References

- [Arc10] J. Archibald, *The multivariable Alexander polynomial on tangles*, PhD thesis, University of Toronto, 2010, available at http://www.math.toronto.edu/jfa/jana_thesis.pdf
- [Big12] S. Bigelow, *A diagrammatic Alexander invariant of tangles*, arXiv: 1203.5457v1
- [BL11] J. A. Baldwin, A. S. Levine, *A combinatorial spanning tree model for knot Floer homology*, arXiv: 1105.5199v2
- [Bar02] D. Bar-Natan, *On Khovanov’s categorification of the Jones polynomial*, arXiv: 0201043v3
- [Bar04] D. Bar-Natan, *Khovanov’s homology for tangles and cobordisms*, arXiv: 0410495v2
- [EPV15] A. P. Ellis, I. Petkova, V. Vértesi: *Quantum $\mathfrak{gl}(1|1)$ and tangle Floer homology*, arXiv: 1510.03483v1
- [FJR09] S. Friedl, A. Juhász, J. A. Rasmussen *The decategorification of sutured Floer homology*, arXiv: 0903.5287v4
- [GL86] P. M. Gilmer, R. A. Litherland, *The duality conjecture in formal knot theory*, Osaka Journal of Mathematics. 23, pp. 229–247, 1986
- [Har83] R. Hartley, *The Conway potential function for links*, Comment. Math. Helvetici, no. 58, pp. 365–378, 1983
- [Jia14] B. Jiang, *On Conway’s potential function for colored links*, arXiv: 1407.3081v2.
- [Juh06] A. Juhász, *Holomorphic discs and sutured manifolds*, arXiv: 0601443v3
- [Kau83] L. Kauffman, *Formal Knot Theory*, Princeton University Press, 1983.
- [Ken12] G. Kennedy, *A diagrammatic multivariate Alexander invariant of tangles*, arXiv: 12055781v2
- [OS03] P. Ozsváth, Z. Szabó, *Holomorphic disks and knot invariants*, arXiv: 0209056v4
- [OS07] P. Ozsváth, Z. Szabó, *Holomorphic disks and link invariants*, arXiv: 0512286v2
- [Pol10] M. Polyak, *Alexander-Conway invariants of tangles*, arXiv: 1011.6200v1
- [PV14] I. Petkova, V. Vértesi, *Combinatorial tangle Floer homology*, arXiv: 1410.2161v1
- [Ras03] J. A. Rasmussen, *Floer homology and knot complements*, arXiv: 0306378v1
- [Ras05] J. A. Rasmussen, *Knot polynomials and knot homologies*, arXiv: 0504045v1
- [Srk06] S. Sarkar, *Maslov index formulas for Whitney n -gons*, arXiv: 0609673v4
- [Srt06] A. Sartori, *The Alexander polynomial as quantum invariant of links*, arXiv: 1308.2047v2
- [Weh09] S. M. Wehrli, *Mutation invariance of Khovanov homology over \mathbb{F}_2* , arXiv: 0904.3401v1
- [nb] C. B. Zibrowius, Mathematica notebook `AlexanderTangleInvariant.nb`, submitted with this article, along with a manual for how to use the program
- [rel] C. B. Zibrowius, some notes on relations in Kennedy’s invariant for 4-ended tangles, available at <https://www.dpmms.cam.ac.uk/~cbz20/documents/research/Kennedy4ended.pdf>
- [Zib15] C. B. Zibrowius, *On a polynomial Alexander invariant for tangles*, an essay for the Smith-Knight & Rayleigh-Knight Prize Competition, January 2015, Cambridge, UK

All webpages above have been successfully accessed on 18th January 2016.